Hindawi Publishing Corporation
Advances in Materials Science and Engineering
Volume 2015, Article ID 165631, 21 pages
http://dx.doi.org/10.1155/2015/165631

Review Article

Piezoelectric Nanowires in Energy Harvesting Applications

Zhao Wang,[1] Xumin Pan,[1] Yahua He,[1] Yongming Hu,[1] Haoshuang Gu,[1] and Yu Wang[2]

[1]*Hubei Collaborative Innovation Centre for Advanced Organic Chemical Materials, Faculty of Physics and Electronic Science, Hubei University, Wuhan, Hubei 430062, China*
[2]*Department of Applied Physics and Materials Research Center, the Hong Kong Polytechnic University, Kowloon 999077, Hong Kong*

Correspondence should be addressed to Haoshuang Gu; guhsh@hubu.edu.cn and Yu Wang; apywang@polyu.edu.hk

Received 4 December 2014; Accepted 14 April 2015

Academic Editor: Sule Erten-Ela

Recently, the nanogenerators which can convert the mechanical energy into electricity by using piezoelectric one-dimensional nanomaterials have exhibited great potential in microscale power supply and sensor systems. In this paper, we provided a comprehensive review of the research progress in the last eight years concerning the piezoelectric nanogenerators with different structures. The fundamental piezoelectric theory and typical piezoelectric materials are firstly reviewed. After that, the working mechanism, modeling, and structure design of piezoelectric nanogenerators were discussed. Then the recent progress of nanogenerators was reviewed in the structure point of views. Finally, we also discussed the potential application and future development of the piezoelectric nanogenerators.

1. Introduction

Recently, portable and wireless micro- and nanoscaled devices have been widely used in environmental monitoring, medical implants, defense technology, industrial safety, and personal electronics, such as the nanowire-based gas and chemical sensors [1, 2] and programmable nanowire circuit for nanoprocessors [3]. Until now, most of the micro/nanodevices are still working under the driving of conventional power sources such as the lion batteries. Although the long-term performance and miniaturization of batteries have been largely improved in recent years, the relatively larger size, unavoidable recharging, or replacing process may lead to a lot of problems during the fabrication and operation process. For example, the batteries in heart pacemaker need to be replaced after the 6–11 years' usage, which would make the patient suffering from the surgery and lower their lives' quality. Moreover, hydrogen sensors have already been used for detecting the leakage and concentration of hydrogen gas in many fields such as the nuclear power station and generator sets. The complex power supply lines will lead to high potential hazard and limit the development of wireless sensor networks. Therefore, the development of novel power supply systems without recharging or replacing problems and micro/nanoscaled dimensions has become an attractive topic.

In the ambient environment and industrial process, most of the energies such as optical, heat, mechanical vibration and chemical reaction are wasted. The highly efficient harvesting and conversion of such energies may not only be used for building the self-powered devices, but also promote the development of clean and renewable energy sources. Among them, mechanical energy is abundant in the environment, including the mechanical vibration, hydraulic pressure, air flow and rain drops. They can be harvested and converted into electric output energy through the "piezoelectric effect," which is so called "piezoelectric electricity generation." Actually, this effect has already been practically used in macroscale devices. For example, by installing piezoelectric bulk materials such as $Pb(Zr,Ti)O_3$ (PZT) ceramics and $Pb(Mg,Nb)O_3$-$PbTiO_3$ (PMN-PT) crystals under the highways, the pressure from the moving vehicles can be converted into electric powers, which is strong enough to illuminate the caution lights on the highways.

In the last decade, the development on the synthesis technique of the piezoelectric nanomaterials has promoted the miniaturization of the piezoelectric generators [4, 5].

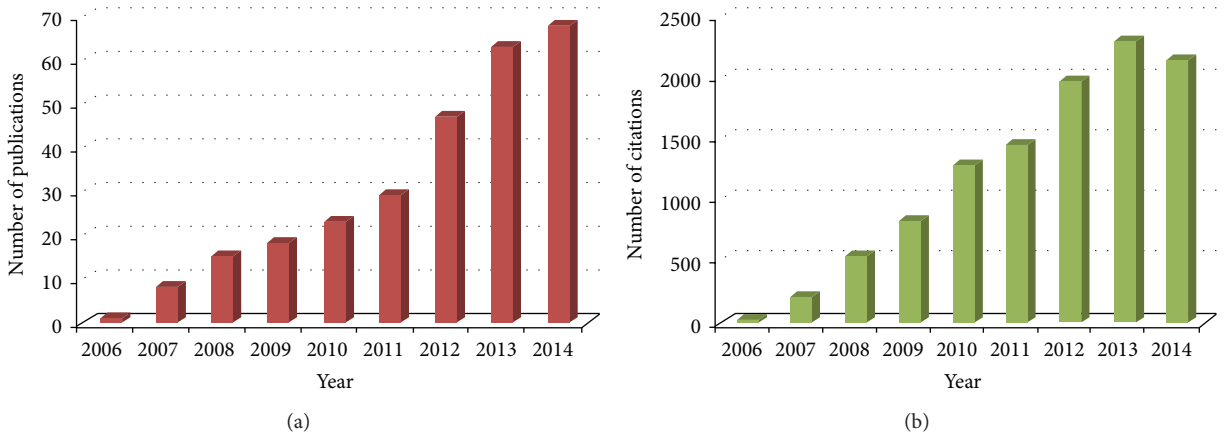

Figure 1: Publication (a) and citation (b) about the piezoelectric nanogenerators according to the data enquired in Thomson Reuters ISI Web of Knowledge.

Wang and Song firstly reported the piezoelectric "nanogenerators" in 2006, which can generate impulsive output voltage with several millivolts by bending a ZnO nanowire with the atomic force microscopy (AFM)'s tip [6]. This nanogenerator has attracted great interest of researchers due to the great potential in the application of micro/nanoscaled power supply systems. However, the energy conversion efficiency and output power of this early-stage device are too low to be applied. In the last 8 years, researchers have done great efforts on improving the device performance, including the employing of several kinds of piezoelectric materials with higher piezoelectric properties [7–9], the design of device structures [10, 11], and the hybrid of nanogenerators with other types of energy harvesters [12, 13]. Moreover, some novel applications such as the active chemical sensors were also developed by using the nanogenerators [14, 15]. As shown in Figure 1, the publication and citation number of research works have largely increased from the first report in 2006.

In this paper, we firstly reviewed the fundamental theory about the piezoelectricity and piezoelectric materials in Section 2. Then the working mechanism, modeling and structural design, and the fabrication and performance of the piezoelectric nanogenerators based on different structures were discussed. After that, the application of piezoelectric nanogenerators in recent years was briefly reviewed. Finally, the future development of the nanogenerators was also discussed.

2. Piezoelectricity and Piezoelectric Materials

2.1. Definition and Physics of Piezoelectricity. Piezoelectric effect is a unique property of certain crystals where they will generate an electric field or current if subjected to physical stress. The direct piezoelectric effect was discovered by brothers Pierre Curie and Jacques Curie in 1880. After that, the same effect was observed in reverse, where an imposed electric field on the crystal will put stress on its structure.

The process whereby the piezoelectric effect takes place is based on the fundamental structure of a crystal lattice. Crystals generally have a charge balance, where negative and positive charges precisely cancel each other out along the rigid planes of the crystal lattice. When this charge balance is disrupted by applying physical stress to the crystals, the energy is transferred by electric charge carriers, creating a current in the crystal. With the converse piezoelectric effect, the applying of an external electric field to the crystal will unbalance the neutral charge state, which results in mechanical stress and the slight readjustment of the lattice structure. Therefore, piezoelectricity is the linear interaction between the mechanical and electrical properties of the dielectric materials [10]. For electrical properties, the relationship between the electric displacement (D_i) and the electric field (E_j) can be interpreted as

$$D_i = \sum_{j=1}^{3} \varepsilon_{ij} E_j, \tag{1}$$

where the coefficient ε_{ij} is the permittivity of the dielectric materials. The permittivity coefficient is a second-rank tensor represented by a 3×3 matrix. However, the matrix is symmetric ($\varepsilon_{ij} = \varepsilon_{ji}$), and there are at most 6 independent coefficients. For mechanical properties, the relationship between stress and strain under small deformations can be interpreted as

$$T_{ij} = \sum_{k,l=1}^{3} c_{ijkl} S_{kl}, \tag{2}$$

where c_{ijkl} is the elastic stiffness of the material. Equation (2) can also be interpreted reversely as

$$S_{ij} = \sum_{k,l=1}^{3} s_{ijkl} T_{kl}, \tag{3}$$

where s_{ijkl} is the elastic compliance of the materials. Because the stiffness and compliance coefficients relate to the second-rank tensor stress and strain, they are fourth-rank tensors. However, due to the symmetric stress and strain ($T_{ij} = T_{ji}$, $S_{ij} = S_{ji}$), the number of c_{ijkl} can be reduced to 36 [10].

Table 1: Typical piezoelectric material in different category.

Category	Typical materials
Natural crystals	Berlinite ($AlPO_4$), sucrose, quartz, Rochelle salt, topaz, and tourmaline-group minerals
Natural materials	Bone, tendon, silk, wood, enamel, dentin, DNA, and viral proteins
Synthetic crystals	Gallium orthophosphate ($GaPO_4$), langasite ($La_3Ga_5SiO_{14}$), and diisopropylammonium bromide (DIPAB)
Synthetic ceramics	$BaTiO_3$, $PbTiO_3$, $Pb(Zr,Ti)O_3$, $KNbO_3$, $LiNbO_3$, $LiTaO_3$, Na_2WO_3, ZnO, $Ba_2NaNb_5O_5$, $Pb_2KNb_5O_{15}$, and so forth
Lead-free piezoceramics	$(K,Na)NbO_3$, $BiFeO_3$, $Bi_4Ti_3O_{12}$, $Na_{0.5}Bi_{0.5}TiO_3$, and so forth
Polymers	Polyvinylidene fluoride (PVDF)
Organic nanostructures	Self-assembled diphenylalanine peptide nanotubes (PNTs)

In reduced notation, the piezoelectric constitutive equation can be interpreted as [10]

$$D_i = \varepsilon_{ij}^T E_j + d_{iJ} T_J,$$
$$S_I = d_{Ij} E_j + s_{IJ}^E T_J, \tag{4}$$

where the superscripts T and E mean the coefficients are at constant stress and electric field, respectively. The d_{iJ} in (4) is the piezoelectric strain/charge constant. Under the one-dimensional simplified hypothesis, the piezoelectric constitutive equation can also be interpreted as follows:

$$S = s^E T + dE$$
$$D = dT + \varepsilon^T E \tag{5a}$$

$$S = s^D T + gD$$
$$E = -gT + \frac{D}{\varepsilon^T} \tag{5b}$$

$$T = c^E S - eE$$
$$D = eS + \varepsilon^S E \tag{5c}$$

$$T = c^D S + hD$$
$$E = -hS + \frac{D}{\varepsilon^S}. \tag{5d}$$

Among them, d, e, g, and h are piezoelectric constant and can be linked as

$$d = \varepsilon^T g = s^E e$$
$$e = \varepsilon^S h = c^E d$$
$$g = \frac{d}{\varepsilon^T} = s^D h \tag{6}$$
$$h = \frac{e}{\varepsilon^S} = c^D g$$
$$\varepsilon^T = \varepsilon^S + de.$$

2.2. Typical Piezoelectric Materials. Until now, several kinds of materials have exhibited piezoelectricity including both natural and synthetic materials, which are listed in Table 1. Among them, piezoelectric ceramics, crystals, and polymers were most developed and useful piezoelectric materials. Piezoelectric ceramics usually refer to polycrystalline materials that consisted of irregular collective small grains and are prepared through the solid-state reaction and sintering process. Under the poling electrical field, the disordered spontaneous polarization in piezoelectric ceramics can be realigned and keep the remnant polarization after the removal of external field. As a result, the piezoelectric ceramics can exhibit macropiezoelectric property. Piezoelectric crystals, which refer to single-crystalline materials, are usually unsymmetrical in structure and therefor exhibit piezoelectric property.

The piezoelectric ceramics exhibit high piezoelectric constant and permittivity and can be prepared into designed architectures, which makes them suitable for the application in high-power energy transducer and wideband filters. However, the poor mechanical quality factor, high electrical loss, and low stability of the piezoelectric ceramics limited their application in high-frequency devices. Comparatively, the natural piezoelectric crystals such as quartz exhibit lower piezoelectric properties and dielectric constant. Moreover, they are limited in size due to the cuts of crystals. However, the mechanical quality factor and stability of quartz crystals are relatively higher than ceramics. Therefore quartz crystals are always used in high-frequency filters, transducers, and other standard frequency controlling oscillators. Besides the quartz crystals, the high-quality perovskite piezoelectric single crystals such as the $Pb(A_{1/3}B_{2/3})O_3$-$PbTiO_3$ (A = Zn^{2+}, Mg^{2+}; B = Nb^{5+}) with much higher piezoelectric constant (d_{33} ~ 2600 pC/N), electromechanical coupling coefficient (k_{33} ~ 0.95), and strain (>1.7%) have also been obtained since 1997 [16, 17]. These single crystals are new-generation piezoelectric materials for high performance piezoelectric devices and systems including ultrasound medical imaging probes, sonars for underwater communications, and sensors/actuators. However, the size and shape of the piezoelectric single crystals are difficult to be preciously controlled during the growth process, which limit the practical application in many fields such as the microscaled actuators and composite metamaterials.

Furthermore, the piezoelectric polymers such as polyvinylidene fluoride (PVDF) with high flexibility, low density,

and resistance as well as relatively higher piezoelectricity voltage constant (g) have also attracted much attention in recent years [18, 19]. Unlike the piezoelectric ceramic and crystals, the intertwined long-chain molecules in polymers attract and repel each other when an electric field is applied. PVDF has exhibited great potential in the application of acoustic ultrasound measurements, pressure sensors, and ignition/detonations. However, the relatively low piezoelectric strain constant (d) of PVDF limited the application in transducers.

2.3. Applications of Piezoelectric Materials. Nowadays, piezoelectric materials have been widely used in the industrial, manufacturing, automotive industry, and medical instruments as well as information and telecommunication fields, and so forth. According to the operation mode of the piezoelectric devices, the application of piezoelectric materials can be classified as follows.

(1) Sensors. Through the direct piezoelectric effect, the piezoelectric materials can be used for the detection of pressure variations in longitudinal, transversal, and shear modes. The most commonly used application of piezoelectric sensors is in the sound form, such as the piezoelectric microphones, piezoelectric pickups in acoustic-electric guitars, and detection of sonar waves. Moreover, the piezoelectric sensors can also be used with high-frequency field such as the ultrasonic medical imaging or industrial nondestructive testing. In addition, the piezoelectric sensors were also employed in piezoelectric microbalance and strain gauges.

(2) Actuators. On contrary to piezoelectric sensors, the working of actuators is usually based on the reverse piezoelectric effect to induce tiny changes in the width of the piezoelectric materials by applying high electric fields. Due to the relatively high precision of the width changes, the piezoelectric actuators are always used in accurate positioning. For example, the piezoelectric motors with high accuracy have already been used in optical devices, transportation and aerospace techniques, robots, medical devices, biology, and nanomanipulation fields, such as the atomic force microscopes (AFM), scanning tunneling microscopes (STM), autofocusing camera lens, inkjet printers, CT/MRI scanners, and X-ray shutters.

(3) Frequency Controlling Devices. Crystal oscillator is an electronic oscillator circuit that uses the mechanical resonance of a vibrating piezoelectric crystal to create an electrical signal with a very precise frequency. The frequency can be used to provide a stable clock signal for digital integrated circuits. Moreover, the piezoelectric materials have also been used in high-frequency resonators and filters, such as the surface acoustic wave devices and film bulk acoustic resonators.

(4) High Voltage and Power Sources. By applying the external mechanical stimulates, the piezoelectric ceramic or crystals can generate potential differences with thousands of volts in amplitude. Therefore, piezoelectric materials can be used as high voltage and power sources. The most commonly application is the piezoelectric ignition/sparkers such as the cigarette lighters. Moreover, the piezoelectric materials have been employed for energy harvesting applications. For example, the energy from human movements and vehicle movements in public places can be harvested and converted into electricity for lighting the lamps. Recently, the microscale energy harvesters were developed for harvesting the small-scale mechanical energies by using the piezoelectric nanomaterials, which is called "piezoelectric nanogenerators." The nanogenerators can be used for charging the batteries or directly driving some low-power microdevices. The recent progress of piezoelectric nanogenerators will be reviewed in the next section.

3. Piezoelectric Nanowires for Energy Harvesting Applications

The first research work about the piezoelectric nanogenerators was reported by Wang and Song in 2006. After that, numerous research works have been conducted about the working mechanism, structural modeling and design, and performance optimization of the piezoelectric nanogenerators. Until now, several kinds of flexible nanogenerators have been developed, which could be used for harvesting that varies mechanical energies from the environment or human bodies. The output electrical energy has been increased from several millivolts to several hundred volts, which is enough for driving a light-emission diode (LED), liquid crystal display (LCD), and wireless data transmitting device. In this section, the author briefly reviewed the working mechanism, modeling/simulations, and the experimental progress of piezoelectric nanogenerators according to the structure of the nanogenerators including the vertical-aligned nanowire arrays, the lateral-aligned nanowire networks, and the nanowire-based nanocomposites.

3.1. Vertical-Aligned Nanowire Arrays

3.1.1. Working Mechanism and Structural Modeling. Two different working models can be used for describing the working process of the nanogenerators based on vertical-aligned nanowire arrays including the lateral bending and vertical compression. Due to their different electrical and mechanical configurations, the working mechanism is different in certain degrees, but with one consistent basis: the coupling of the semiconductor behavior and the piezoelectric property of the piezoelectric nanowire.

Figure 2 illustrated the working mechanism of the nanogenerator based on a bending nanowire induced by an AFM tip [20]. As shown, a Schottky barrier was built up between the nanowire and the AFM tip due to the difference of working function and electron affinity. The system was in an equilibrium state and no voltage output was generated when the nanowire is not bent by the AFM tip. Once the nanowire was bent by the scanning AFM tip, the asymmetric piezoelectric potential would be generated due to the stretch and compression of the inner and outer side of the nanowire. The piezoelectric potential in the nanowire changed the

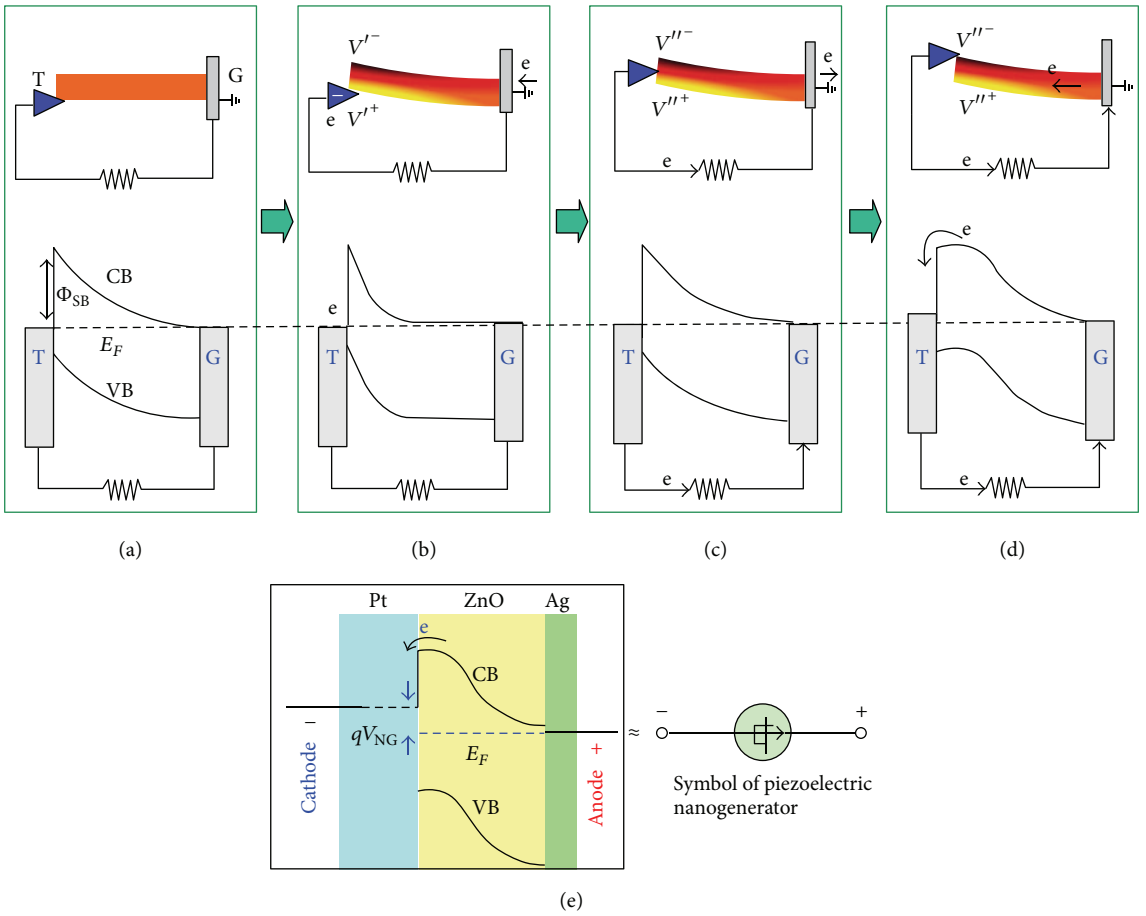

FIGURE 2: The band diagram for understanding the charge output and flow processes in a nanogenerator with lateral bending model. (a) Before bending; (b) nanowire bent by the tip with the tip point at the stretched surface; (c) tip scans across the nanowire and reaching the middle point; (d) tip reaching the compressed surface of the nanowire; (e) energy-band diagram for the nanogenerator, presenting the output voltage and the role played by the piezoelectric potential. (Reproduced from [20] with the permission from WILEY-VCH Verlag GmbH & Co. KGaA, Weinheim.)

profile of the conduction band. As shown in Figure 2(b), the local positive piezoelectric potential at the contact area would lead to a slow flow of electrons from ground to the tip through the external load, which resulted in the charge accumulation in the tip. When the tip was moved to the middle part of the nanowire, the local potential dropped to zero and resulted in a back flow of the accumulated electrons through the load to the ground (Figure 2(c)). After that, if the tip was moved to the compressive part of the nanowire, a local negative piezoelectric potential would raise the profile of the conduction band and led to an electron flow from the *n*-type ZnO to the tip. Therefore, a circular flow of electrons would be generated and exhibited output current in the measurement devices [23].

For nanogenerators with vertical compressed nanowire arrays, the piezoelectric nanowires were connected by a pair of electrodes on the top and bottom end with at least one Schottky contact in the interface. The compressive deformation was induced symmetrically along the longitude of the nanowires. As a result, the piezoelectric potential should be well-distributed along the axial direction of the nanowire. Therefore, its working mechanism was different from the bending models. As shown in Figure 3, the alternative electric output could be attributed to the back and forth flow of electrons in the external circuit driven by the piezoelectric potential [23, 24]. Without the external stress, the system was in an equilibrium state and no voltage output would be generated (Figure 3(a)). Once the nanowire was compressed by external force, the piezoelectric potential would be induced along the nanowire. Consequently, the conduction band edge and Fermi level of the negative-potential side would be raised by the piezoelectric field as shown in Figure 3(b). Due to the Schottky barrier on both sides of the nanorod, the electron could not pass through the interface between the nanowire and electrodes to compensate the energy difference and would flow through the external circuit to the electrode on the counter side. Therefore an impulsive electric output would be generated. The electrons were then accumulated due to the Schottky barrier and reached an equilibrium state with the piezoelectric field to make the Fermi energy back to the same

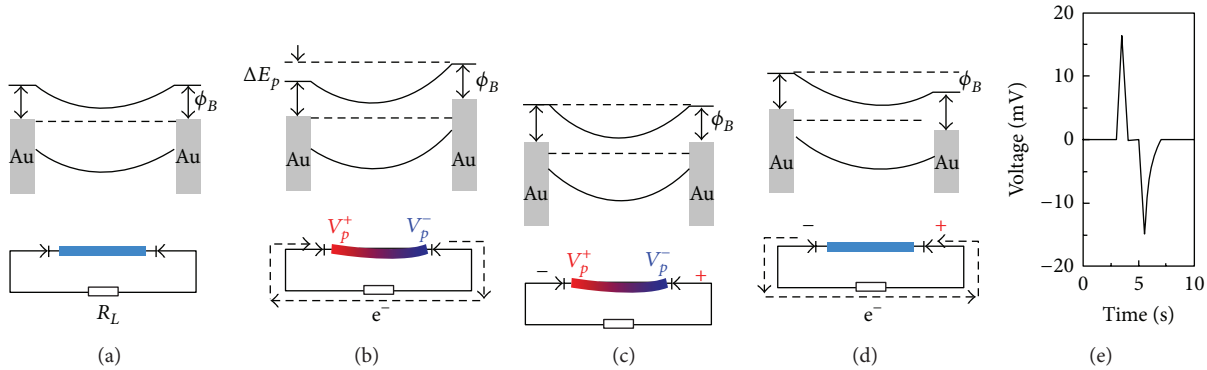

FIGURE 3: Band diagram for understanding the charge output and flow process in the nanogenerator with compressed nanowire. (a) Before pressing. (b) Nanowire vertically compressed by external force. (c) Equilibrium state under strain state. (d) Release of pressure. (e) Output voltage.

level, which led to no more electrical output in the external circuit (Figure 3(c)). When the compression was released as shown in Figure 3(d), the piezopotential was vanished, which would break the equilibrium state. Therefore, the energy difference would be induced on the opposite direction and lead to an impulsive negative electrical output signal.

Because of the complex and expensive fabrication and characterization and integration process of piezoelectric nanogenerators, the accurate modeling and performance simulation about the electromechanical conversion behavior of the nanowires were important before the experimental works. For example, Falconi and coauthors have conducted finite element method (FEM) simulation works to estimate the output potential and stored electrostatic energy of a ZnO nanowire under various deformation configurations with different positions of the contacts [10, 11]. In order to simplify the FEM modeling process, the nonlinear behavior of Schottky contact, uncertain load in the external circuit, nonzero electrical conductivity of piezoelectric materials, and parasitic effects were neglected. The simulation was simplified as to qualitatively compare the static piezoelectric potential generated by nanowire with different structure. Their simulation result suggested that the electrode contact configuration would have great impact on the piezoelectric potential of a bending nanowire. Because the highest strain was distributed at the bottom regain of the nanowires, the highest piezoelectric potential difference between the electrodes can be obtained when the electrodes were set up on both sides at the bottom of the nanowire. However, it is difficult to obtain this kind of nanoscaled electrodes in practical experiments. They also compared the performance of bending nanowires with the vertically compressed nanowires and found that the latter one exhibited higher energy conversion efficiency than the bending nanowires with the same electrode configurations. According to their results, the vertical compression model with relatively higher electrical output and simplified structures is more suitable for the practical applications than the bending models. However, the influence of free charge in the nanowires to the electromechanical conversion efficiency was not considered in this work, which has been reported to be a key issue for the piezoelectric nanogenerators.

Recently, the polarization screening effects induced by the free charge carriers have been regarded as an important issue for optimizing the electromechanical conversion efficiency of the piezoelectric nanowires. However, it was very difficult to precisely control the concentration of dopant in piezoelectric nanowires in practical experiments. Therefore, the computer analysis through FEM can be used to predict this effect. For example, Gao and Wang have investigated the behavior of free charge carriers in a bent piezoelectric semiconductive nanowire under thermodynamic equilibrium conditions [25]. They found that the positive side of the bent nanowire would be partially screened by the free charge carriers because the conduction band electrons would be accumulated at the positive side under the piezoelectric potential. Therefore, the potential in positive side is much lower than the negative side. Moreover, Falconi et al. have investigated the screening effect in a vertically compressed nanowire and found that the piezoelectric potential would be almost completely screened by the free charge carriers at a higher level of donor concentrations. They also confirmed that the length of the vertically compressed nanowire did not significantly affect the maximum value of the piezoelectric potential, while the relative dielectric constant surrounding the nanowire would significantly influence the output voltage [26].

3.1.2. Fabrication and Performance of Vertical Integrated Nanogenerators. After finding that the AFM tip-induced lateral bending of nanowire (ZnO, GaN, CdS, InN, and ZnS) can generate impulsive voltage output [27–31], another kind of nanogenerator with similar mechanism was carried out. In this device, the AFM tips were replaced by a zigzag top electrode to bend the nanowires [32]. Qin et al. have also reported a similar nanogenerator with two fibers coated by the ZnO nanowire arrays [21]. As shown in Figure 4, they entangle the fibers and brush the nanowires with each other to make the ZnO nanowires bending. This nanogenerator can generate voltage with approximately 1 mV in amplitude. Although these early-stage nanogenerators have attracted a lot of attention, the complicated fabrication process as well as

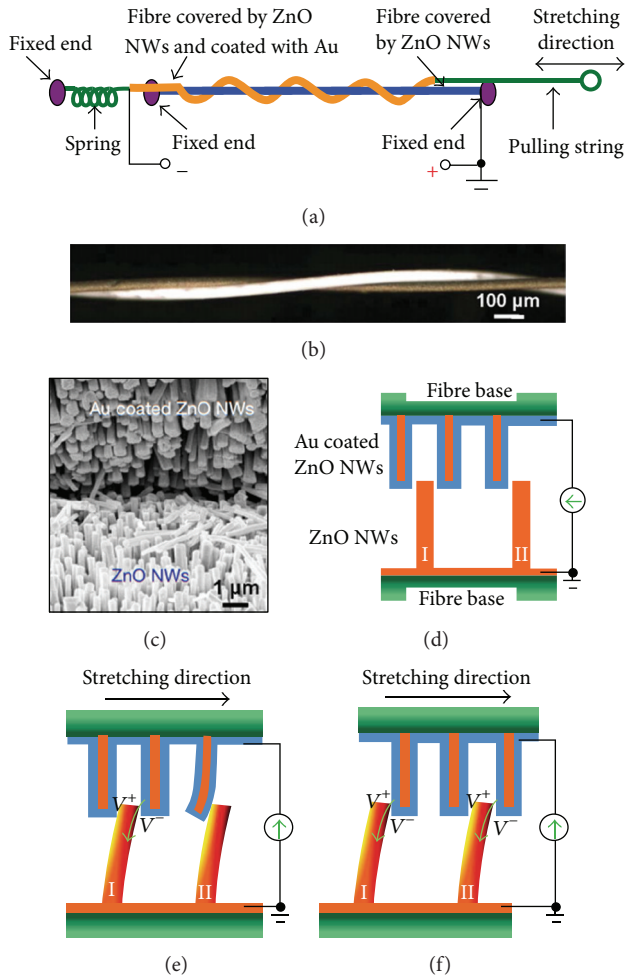

FIGURE 4: Design and electricity-generating mechanism of the fibre-based nanogenerator driven by a low-frequency, external pulling force. (Reproduced from [21] with the permission of Nature Publishing Group).

the low electrical output and poor stability makes them not suitable for practical application.

According to the modeling discussed above, the vertical compress of nanowires could generate higher output voltage than the top-bottom contacted bending nanowires. Xu et al. have fabricated a vertical nanowire array integrated nanogenerator (VING) [33]. As shown in Figure 5, the device was fabricated by packaging the vertical-aligned ZnO nanowire array with polymethyl methacrylate (PMMA) and connected the nanowire with top-bottom flat electrodes, which can generate several tens of millivolts in amplitude under external pressures. The fabrication process of the VING is much simpler than the bending type nanogenerators. Moreover, the packaging of PMMA can largely increase the robustness of the devices. Due to the easy synthesis process of ZnO nanowire arrays, ZnO VING has become the most popular design among the reported nanogenerators. Several improvements have been carried out by researchers. For example, Kim et al. have demonstrated a ZnO VING based on cellulose paper substrates, which could increase the thermal stability of the VINGs [34]. Choi and coworkers have reported a ZnO VING based on transparent and flexible graphene electrodes [35]. The nanogenerator can be fully rolled for the energy harvesting and converting process. The output current of this device is up to 2-3 mA/cm^2 under nonrolling and rolling state. Besides the conventional VINGs, some novel designs on the architecture of VINGs have been demonstrated by researchers. For example, Hu et al. have fabricated a ZnO VING which is a free-standing cantilever beam made of a five-layer structure [36]. By depositing the ZnO seed/Cr layers on the top and bottom surfaces of the polyester (PS) substrate, the densely packed ZnO nanowire texture films were synthesized and then covered by PMMA as blocking layer. Finally, the top electrodes were deposited on top of both PMMA layers, and the whole system was packaged by PDMS. The layered VINGs can generate open-circuit voltage up to 10 V and short-circuit current up to 0.6 μA, when it was strained to 0.12% at a strain rate of 3.56%/s.

As mentioned above, the free charges in n-type ZnO nanowires will screen the piezoelectric potential. That will decrease the output voltage of the ZnO nanogenerators.

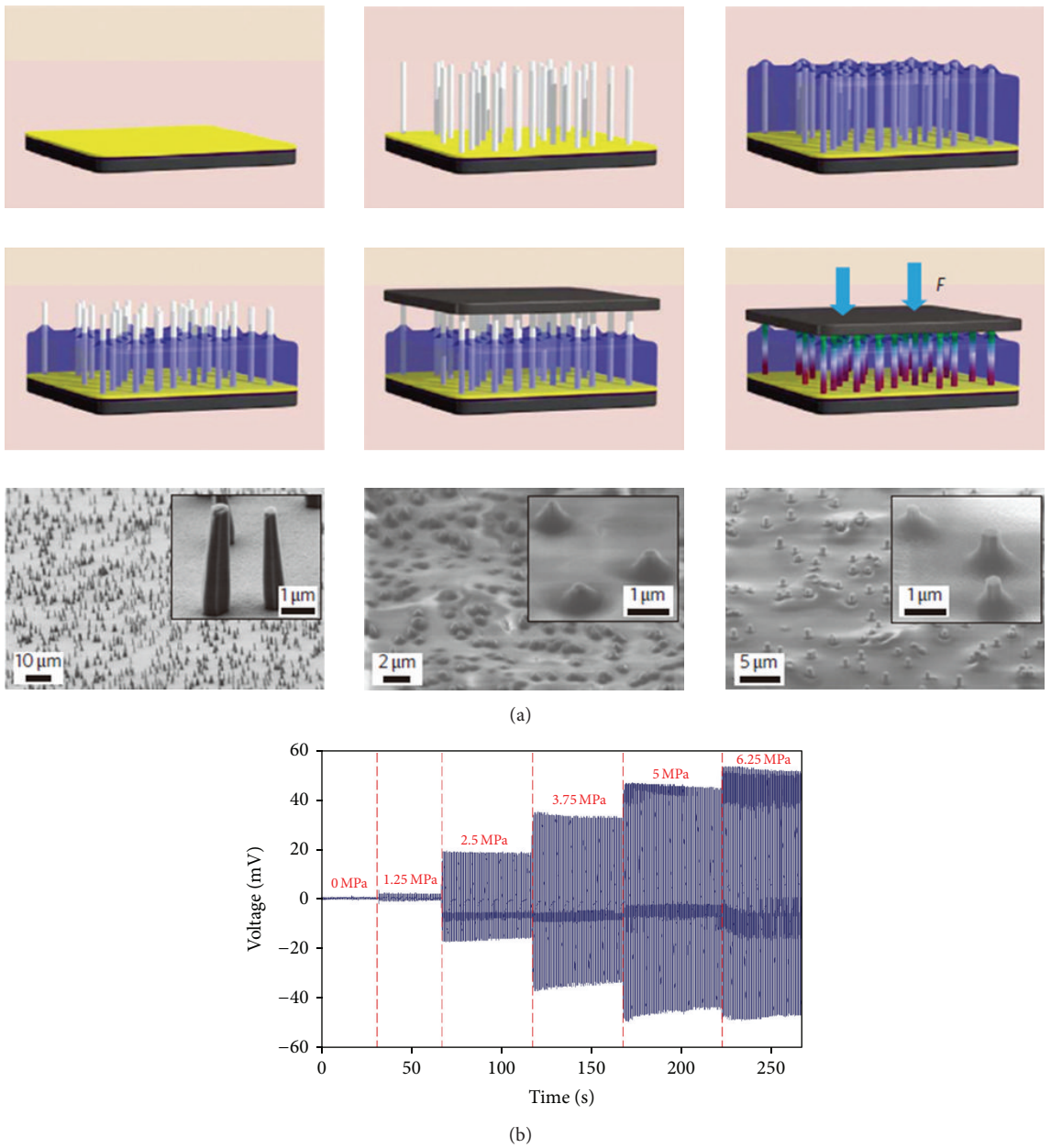

FIGURE 5: (a) Schematic diagram of the fabrication process of the VING. (b) The output voltage of the VING under different external pressures. [Reproduced from [22] with the permission from Nature Publishing Group.]

Until now, two major approaches have been employed for decreasing of the screening effect. Firstly, it can be realized by improving the intrinsic properties of ZnO through pretreatment and surface passivation, and so forth. For example, Hu et al. have improved the single-layered VINGs' performance with maximum output voltage up to 20 V and output current up to 6 μA by treating the ZnO nanowires with oxygen plasma or annealing in air [37]. Moreover, the output performance of the ZnO nanorod based nanogenerators could also be improved by inducing the ultraviolet light to passivate the surface [38]. A similar work was also reported by Lin et al., where the output of CdS nanowire can be modified by using a white light stimulation [27]. Secondly, the screening effect could also be suppressed by changing the structure of the devices. For example, Zhu and coworkers have reported a novel design of ZnO VING [39]. It could generate high electrical output (V_{OC} = 58 V, I_{SC} = 134 μA) due to the new structures due to the thin layer of PMMA between the top of the nanowires and the top electrodes, which could provide a potential barrier of infinite height. The barrier could prevent the induced electrons in the electrodes from internal leaking through the interface between metal and semiconductor. The segmentation of nanowire arrays also guaranteed that the native free-charge carriers within the

nanowires that are not directly compressed will be isolated from the compressed nanowires (Figure 6). This part of the nanowires will not be involved in the screening effect and preserving the piezoelectric potential from further degradation. Besides the structure design, some other method such as the treatment to the piezoelectric nanowire could also decrease the screening effect.

As known, the piezoelectric constant is critical for the electromechanical conversion efficiency of the piezoelectric nanowires. The relatively low piezoelectric constant of ZnO limited the performance of the nanowire in the VINGs. Perovskite piezoelectric materials such as $Pb(Zr,Ti)O_3$ (PZT) exhibited much higher piezoelectric constant than ZnO materials, which may lead to higher energy conversion efficiency and electric output of the nanogenerators. For example, the PZT nanowire array could generate higher output voltage than the ZnO nanowires with the same device architectures [40]. However, the difficult synthesis process of the perovskite nanowire arrays has limited the research and development of such kind of nanogenerators. The flexibility was also limited by the substrate used for material growth (e.g., $Nb:SrTiO_3$ single crystals). Gu et al. have provided a feasible way to overcome the problem of flexibility, where the ultra-long PZT nanowire arrays were fabricated by stacking the lateral-aligned PZT nanofibers layer by layer and connected by top-bottom electrodes [7]. This device produced ultra-high output voltage up to 209 V together with the current density of 23.5 $\mu A/cm^2$, which could instantaneously power up a commercial LED without any energy storage unit. Moreover, Kang and coworkers have reported a lead-free piezoelectric nanogenerator based on vertically aligned KNN nanorod arrays. The nanogenerator exhibited a stable high power density of ~101 $\mu W/cm^3$ [41].

3.2. Lateral-Aligned Nanowire Networks

3.2.1. Working Mechanism and Structural Modeling. In this type of devices, the deformation of the nanowires was always induced by the laterally bending of the nanowires either through the bending of substrate or through the pressure applied along the radical direction of the nanowires. Unlike the local bending of nanowires in the vertical-aligned nanogenerators, the nanowires were uniformly bent in these processes. Due to the ultra-high aspect ratio of the one-dimensional nanostructure, the uniform lateral bending behavior of the nanowires can be regarded as the lateral stretching by neglecting the strain distribution along the radical direction. Therefore, the working mechanism of the nanogenerators based on lateral-aligned nanowires was the same as the compressed nanowires mentioned in the above section.

In Falconi's work, they also compared the energy conversion behavior of the laterally stretched nanowire with the vertically compressed ones [26]. They have found that the laterally bent nanowire can generate higher output voltage than the later one. However, the external forces were directly applied on the nanowires. In practical devices, the nanowires were usually packaged by soft polymers such as PDMS silicone to protect them from the physical damage. The external forces need to be applied on the packaging layers rather than on the nanowires. Therefore the distribution of the applied forces on the nanowires will be different. As a result, the influence induced by the packaging layer should be taken into account during the modeling of the nanogenerators. Figures 7 and 8 show the modified models of nanogenerators with silicone packaging layers for vertical and lateral packaged devices, respectively. The silicone is 10 μm in thickness and 150% in width comparing with the diameter of the nanorod. In vertically compressed model, the nanorod was vertically standing, fixed at the end, and packaged by the silicone. An external force along the axial direction of the nanorod was applied on the top surface of the silicone. Under the compressing force, the nanorod was vertically compressed and generated a piezoelectric potential of ~350 mV between the top surface and the bottom surface.

In lateral stretching model, the nanorod with the same piezoelectric parameters was laterally positioned between two Au electrodes and packaged by the silicone. The pressure was applied on the top surface along the radial direction of the nanorod. As shown in Figure 8(c), the nanowire was bent under the radial compressing force. The piezoelectric potential difference can be calculated to be ~2.74 V by integrating the electric field along the axial direction of the nanorod. These results indicated that the lateral assembled nanorods can generate much higher piezoelectric potential than the vertical assembled ones under the same external pressure, which may provide the insight for the design of piezoelectric nanogenerators.

3.2.2. Fabrication and Performance of Laterally Integrated Nanogenerators. The first lateral type of piezoelectric nanogenerator is reported by Wang and coauthors in 2007 [44]. This device is based on the voltage generation of an individual $BaTiO_3$ nanowire under periodic tensile mechanical load, which is fabricated by placing a $BaTiO_3$ nanowire onto a piezoelectric flexure stage by using nanomanipulation technique. The lateral strain was applied by moving the mobile base of the stage by using a piezo stack driving by external voltage, fixing the other base. The fabrication process of the flexure stage is complex and expensive due to the small dimension. On the contrary, lateral nanogenerators based on flexible polymer substrates such as the polyimide (PI) films have exhibited much simpler fabrication process and higher performance.

Yang et al. have reported a laterally integrated nanogenerator (LING) based on laterally packaged piezoelectric fine wires [42]. The ZnO fine wire lying on the PI substrate was fixed to electrodes at both ends. The bending of the substrate would result in a stretch behavior of the wire and lead to a drop in the piezoelectric potential along the wire. Therefore, an impulsive and alternative output would be generated by the charge flow in the external circuit. The nanogenerator based on single fine wire can generate output open-circuit voltage and short-circuit current of 60–70 mV and 1000–1100 pA in peak to peak amplitude, respectively.

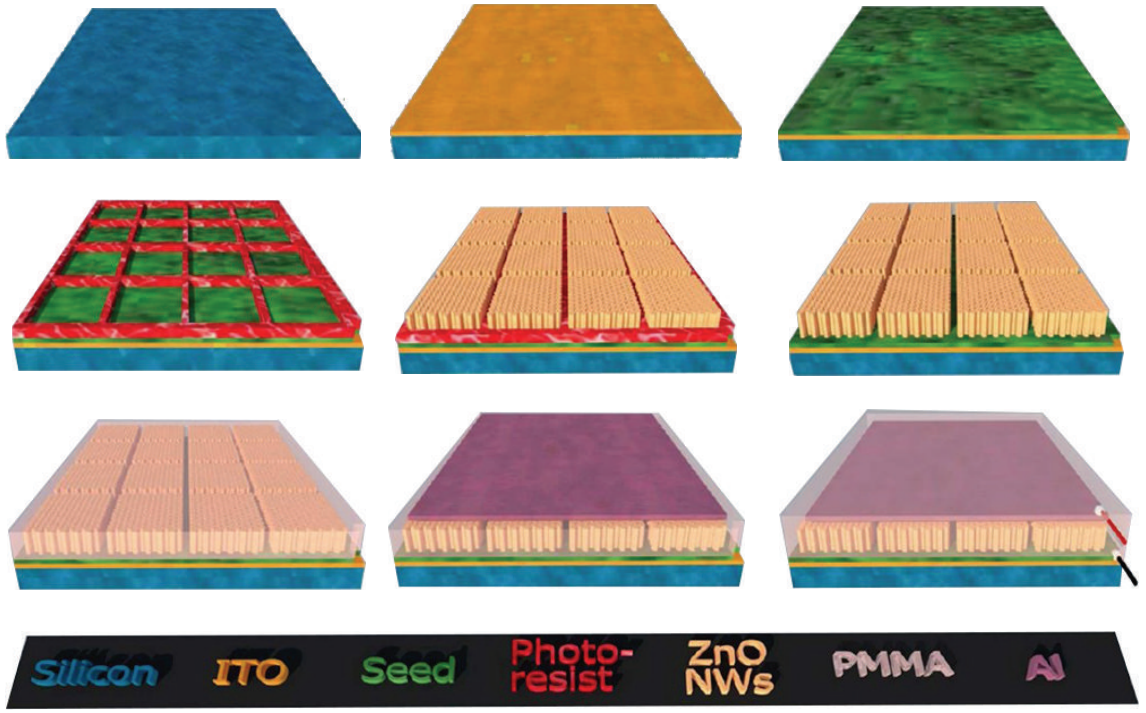

(a)

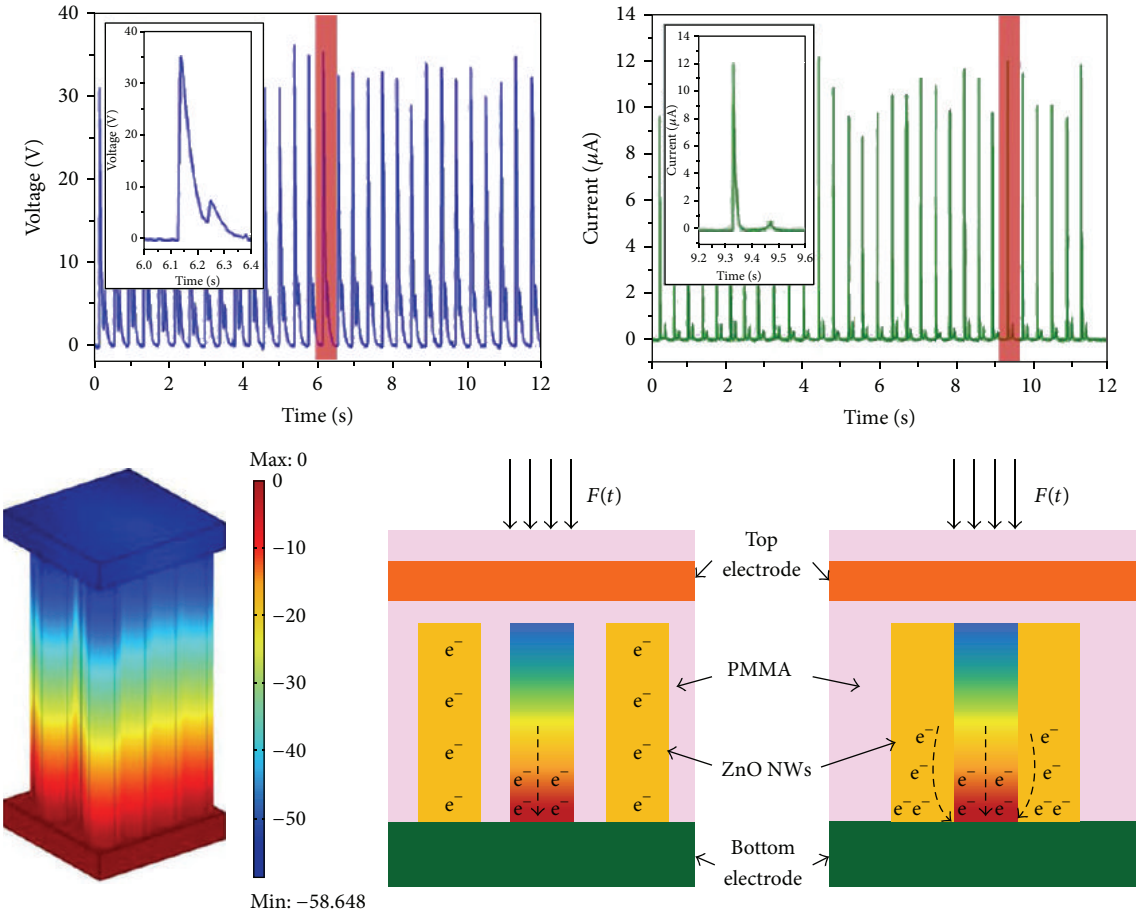

(b)

FIGURE 6: (a) The fabrication process of the segmented ZnO nanowire VINGs. (b) The generated electrical signal and FEM simulation results. [Reproduced from [39] with the permission of American Chemical Society.]

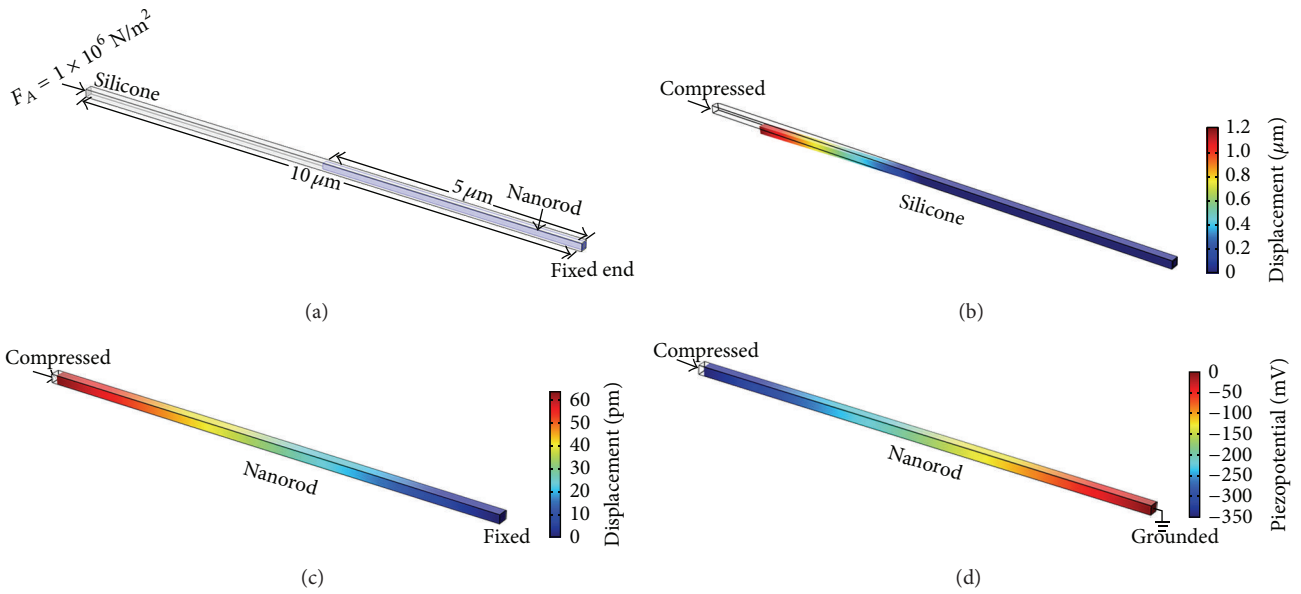

FIGURE 7: FEM static simulation of the electromechanical conversion behavior of a vertically compressed device. (a) Schematic diagram of model. (b) The deformation of silicone. (c) The deformation of nanorod. (d) The piezoelectric potential of nanorod.

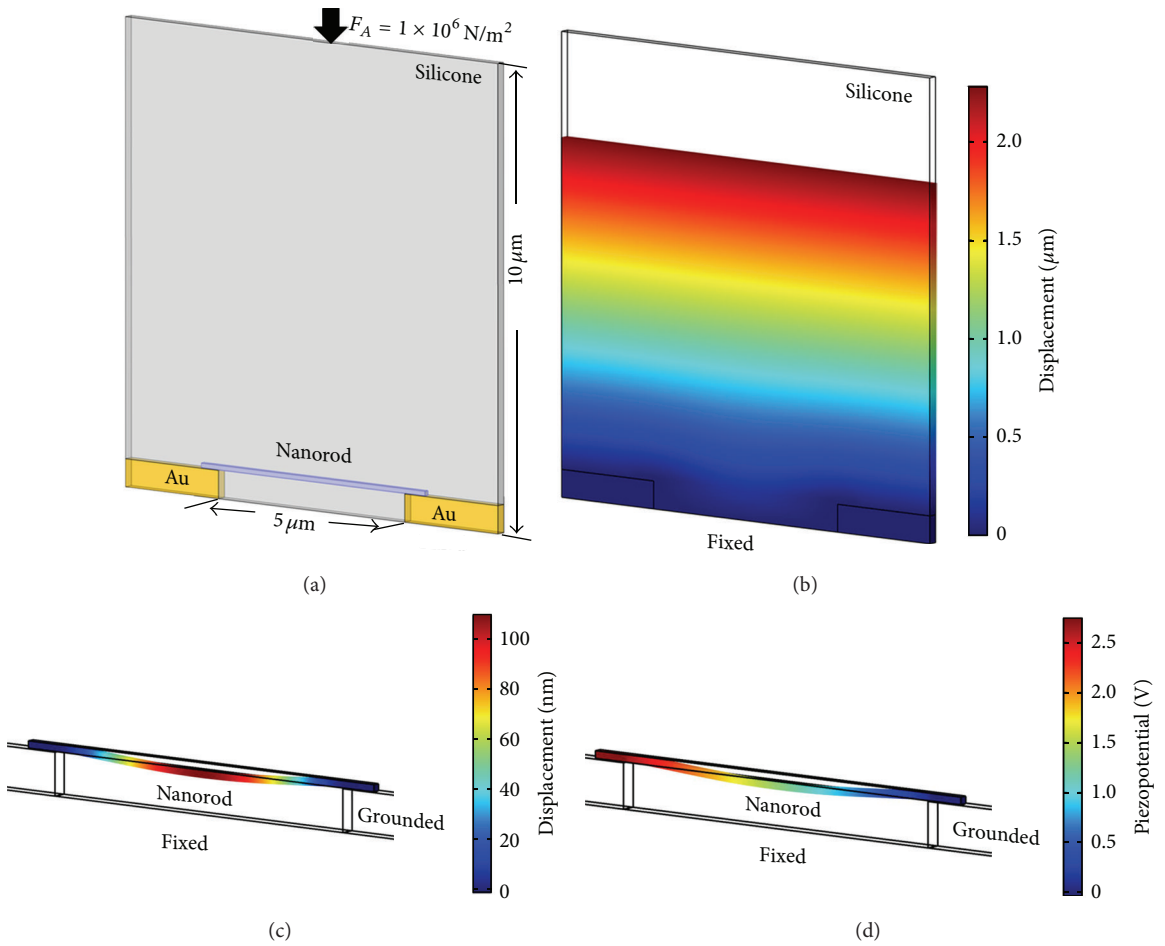

FIGURE 8: Static simulation of the electromechanical conversion behavior of a lateral stretch device. (a) Schematic diagram. (b) Deformation of silicone. (c) Deformation of nanorod. (d) Piezoelectric potential of nanorod.

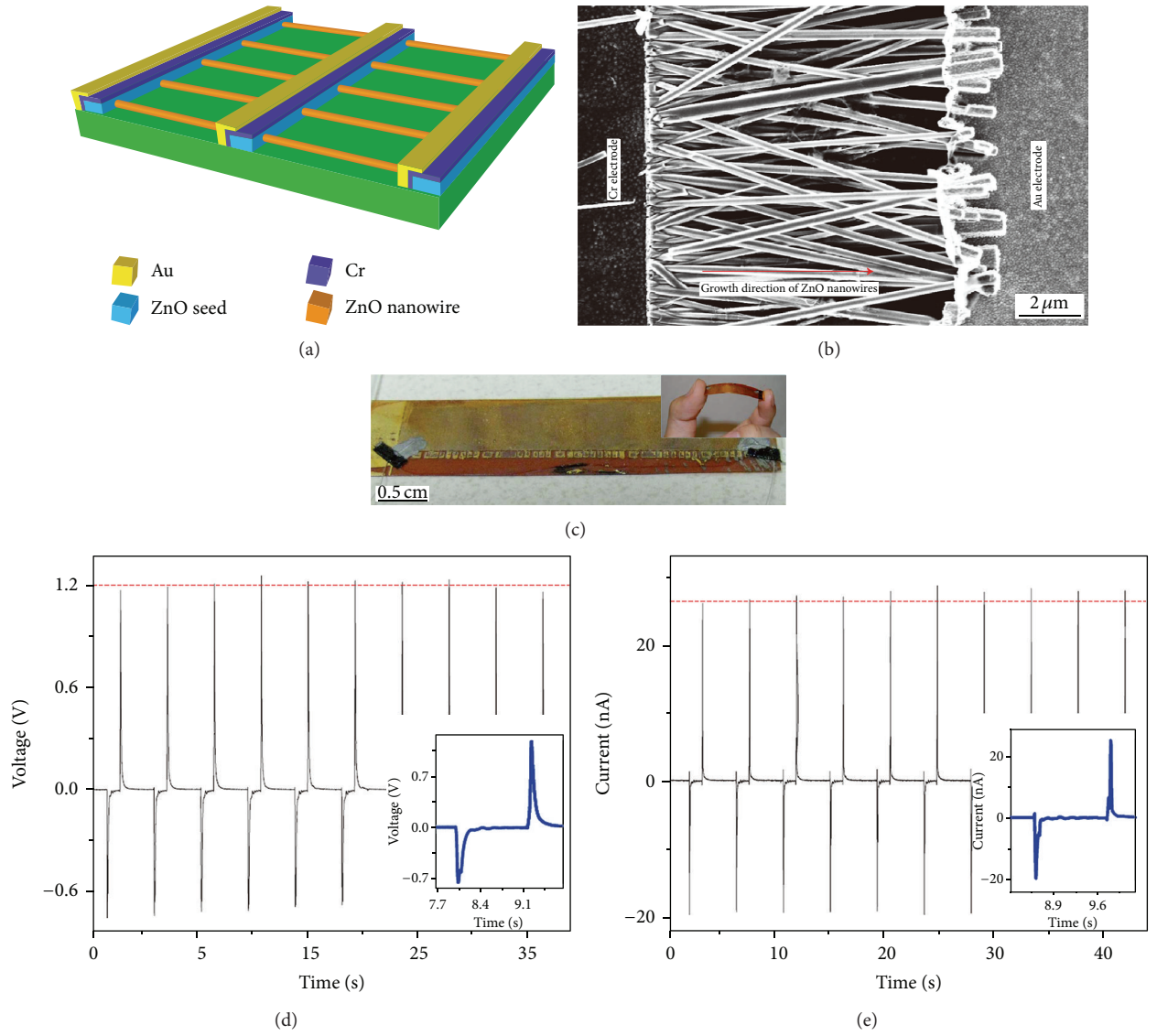

Figure 9: The structural characterization and output performance of the ZnO LINGs. (a) Schematic diagram. (b) Local SEM image; (c) Photograph of a packaged device. (d) Output open-circuit voltage. (e) Output short-circuit current. (Reproduced from [42] with the permission from Nature Publishing Group.).

Moreover, the potassium sodium niobate (KNN) nanorod-based LINGs were fabricated by our group. As known, the piezoelectric constant of the biocompatible KNN is much higher than ZnO, and the free charge carrier density in KNN is lower than ZnO. The KNN nanogenerators may have higher electromechanical conversion efficiency than ZnO-based nanogenerators. In our KNN-LINGs, the KNN nanorods synthesized by hydrothermal and parallel connected by interdigitated electrodes (IDEs) on a flexible PI substrate. The PDMS packaged KNN LINGs can generate parallel open-circuit voltage of about 0.1 V under finger pressing or bending movements [23, 45]. However, the fabrication process of such devices is complex, which would limit the large-scale fabrication of the nanogenerators.

In order to improve and simplify the fabrication process of LINGs, Zhu and coauthors have carried out a scalable sweeping-printing-method for fabricating flexible devices with ZnO nanowire array, which were connected by parallel stripe type of electrodes [22]. The generated open-circuit voltage was up to 2.03 V due to the series connection of nanowires, while a peak output power density of 11 mW/cm^3 was obtained. Another method for one-step fabrication of ZnO nanowire networks was reported by Xu and coworkers [33]. As shown in Figure 9, the nanowires were directly synthesized between the Au/Cr and Au electrodes by low-temperature chemical method and were oriented-aligned with parallel to the substrate surface. By this direct integration process, more than 700 rows of nanowires can be connected in series to increase the output of the nanogenerator, which is up to 1.2 V in open-circuit voltage and 26 nA in short-circuit current at a strain rate of 2.13%/s and strain of 0.19%.

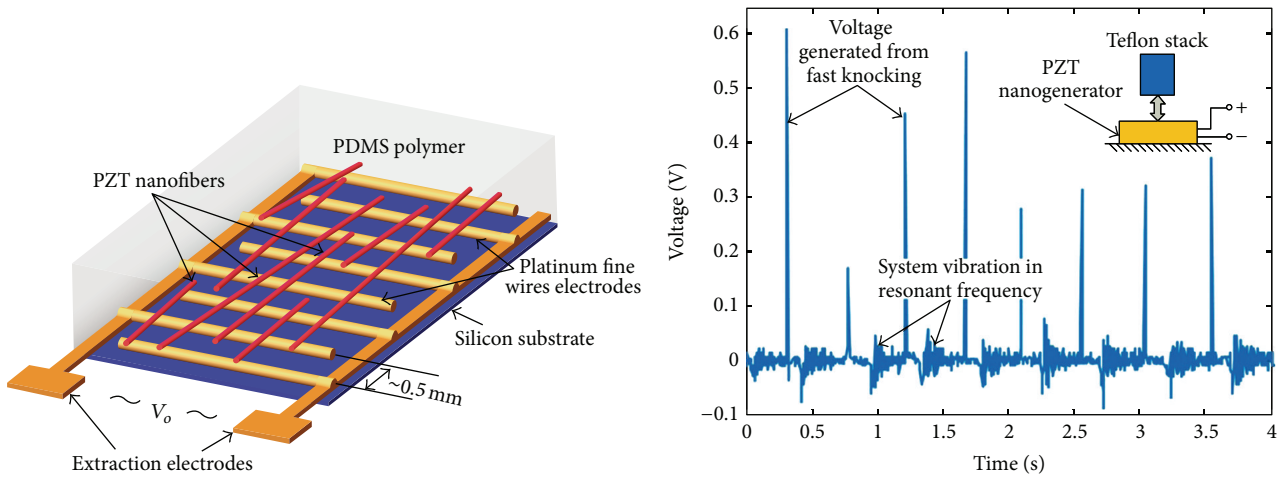

FIGURE 10: The PZT nanofiber-based LING (a) and the generated open-circuit voltage (b). (Reproduced from [43] with the permission from American Chemical Society.)

Recently, the development of electrospinning techniques has promoted the application of the ultra-long piezoelectric nanofibers in the energy harvesting devices, which could also realize the large-scale fabrication of the LINGs [43, 46]. For example, Chen et al. have demonstrated a 1.6 V LING based on electrospun PZT nanofibers [43]. As shown in Figure 10, the PZT nanofibers were directly fabricated on the IDEs by electrospinning and annealing process. After PDMS package and poling, the PZT LING can generate open-circuit voltage up to 1.6 V under the pressure from a Teflon stack or human finger. However, the flexibility of the PZT LING was limited by the substrate due to the high-temperature annealing process. Wu and coauthors have fabricated a PZT textile nanogenerator with parallel-aligned PZT nanofibers transferred from the substrate to a polyethylene terephthalate (PET) film [47]. The wearable LING can generate open-circuit voltage and short-circuit current up to 6 V and 45 nA, respectively. Moreover, the lead-free Mn-doped KNN nanofibers were used for fabricating the flexible LINGs by transferring the annealed KNN nanofibers onto a flexible polyether sulfone (PES) substrate through PDMS. This device exhibited ~0.3 V output voltage and ~50 nA output current under a bending strain [48].

Polyvinylidene fluoride (PVDF) nanofibers were also employed in LINGs. Compared with the inorganic perovskite piezoelectric materials, PVDF nanofibers exhibited better flexibility, lightweight, biocompatibility, and ultra-long lengths, which is more suitable for fabricating biocompatible and flexible nanofiber-based nanogenerators (Figure 11) [46, 57]. As known, the electrospun PVDF nanofibers could transform from nonpolarized α-phase to polarized β-phase structures under the ultra-high electrical field. Chang and coworkers have demonstrated a LING based on a single PVDF nanofiber fabricated by a near-field electrospinning process [58]. Under mechanical stretching, the nanogenerator exhibited repeatable and consistent electrical outputs with energy conversion efficiency higher than the PVDF thin-film based nanogenerators. The open-circuit voltage and short-circuit current of this nanogenerator are 5–30 mV and 0.5–3 nA, respectively. In order to increase the output, they have fabricated 500 parallel nanofibers and connected them with comb-shape electrodes on flexible substrate to amplify the current outputs [59]. The peak current was increased to 35 nA with 0.2 mV in peak voltage. Zhao and co-authors have demonstrated a hybrid LING that consisted of the piezoelectric PVDF nanofibers fabricated by far-field electrospinning process [14]. The PVDF nanofibers were patterned into lateral-aligned arrays on the substrate and were poled with high field (200 kV/cm) for 15 min. The output voltage and current can be increased from 15 to 20 mV and 0.2 to 0.3 nA by increasing the strain rate of the device, respectively. A detailed review about the nanofiber-based LINGs until 2012 was demonstrated by Chang et al. [46]. Moreover, poly(vinylidenefluoride-co-trifluoroethylene) nanofibers have also been employed for high-performance flexible piezoelectric nanogenerators [60, 61]. These devices can also be used for mechanical energy harvesting and ultra-highly sensitive sensing of pressure. Zeng et al. have combined the $NaNbO_3$, PVDF, and the elastic conducting knitted fabric nanofibers to obtain all fiber based nanogenerators, which could generate output voltage of 3.4 V and current of 4.4 μA at 1 Hz and a maximum pressure of 0.2 MPa [62].

3.3. Nanowire-Composite. Recently, a novel type of piezoelectric nanogenerators based on nanowire-polymer composites has attracted researcher's attention. The fabrication process of such devices is much simpler than VING and LING. Basically, the device consisted of four functional layers including the top and bottom electrodes, the flexible substrate, and most importantly the nanowire-composite layer. The multilayer structure of these devices was similar to the piezoelectric

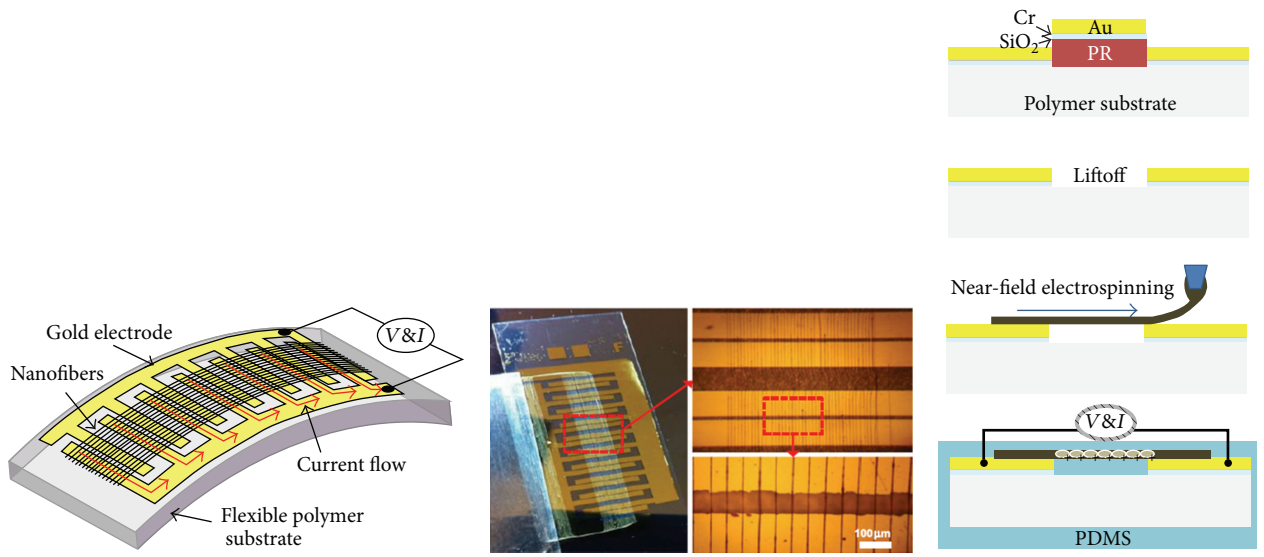

FIGURE 11: Schematic diagram (a), photograph (b), and fabrication process (c) of a PVDF LING. (Reproduced from [46] with the permission from Elsevier.)

TABLE 2: The energy conversion performance of the reported nanogenerators based on nanowire composite.

Piezoelectric materials		Polymer	Output voltage	Strain	Strain rate	Reference
Piezoelectric semiconductor	ZnO nanowires	PMMA	2 V	0.11%	3.67%/s	[49]
	GaN nanowires	PMMA	1.2 V	—	—	[50]
$BaTiO_3$	Nanotubes	PDMS	5.5 V	—	—	[51]
$ZnSnO_3$	Nanobelts	PDMS	5.3 V	0.1%	1.6 Hz	[52]
Lead-free niobates	$NaNbO_3$ nanowires	PDMS	3.2 V	0.23%	12.8%/s	[9]
	$LiNbO_3$ nanowires	PDMS	~0.4 V	0.093% (e_{31}) 0.0168% (e_{33})	—	[53]
	$KNbO_3$ nanowires	PDMS	10.5 V	—	—	[54]
Lead-based piezoelectrices	PMN-PT nanowires	PDMS	7.8 V	—	—	[55]
	PZT nanowires	PDMS	7 V	—	—	[56]

ceramics. Although the piezoelectric properties of the composite may be lower than the ceramics, the polymer matrix largely increased the flexibility of the devices.

For VINGs, the device fabrication was largely limited by the assembly process of the nanowire arrays. Therefore, most of the investigation of VINGs was focused on ZnO nanowire arrays, while LINGs were also suffering from the same problem. However, the nanowire-composite can be easily obtained by directly mixing the as-synthesized nanowires with the polymer matrix such as the PDMS. Therefore, it was a general structure for building nanogenerators. Table 2 listed the reported nanowire-composite nanogenerators with different piezoelectric materials. For example, Hu and coauthors have demonstrated the high output nanogenerators by rational unipolar assembly of conical ZnO nanowires [49]. The macroscopic piezoelectric potential across the thickness of the nanogenerator with output voltage up to 2 V can be produced under a compressive strain of 0.11% at a strain rate of 3.67%/s. A similar structure was also reported by Jung et al. by using $NaNbO_3$ and GaN nanowires composited with PDMS between a pair of electrodes, respectively [9, 50]. The output voltage and current density of the $NaNbO_3$-based device are up to 3.2 V and 72 nA under a compressive strain of 0.23% (Figure 12). Recently, Xu et al. have reported the PMN-PT nanowire-based nanocomposites and nanogenerators [55]. The output voltage and current density of this PMN-PT composite nanogenerator are up to 7.8 V and 4.58 $\mu A/cm^2$. Moreover, PZT nanowires have also been employed for building the nanocomposites nanogenerators and the output voltage was up to 7 V with manual bending. This device can also be used to harvest the energy from the vibration of the cantilevered at the low frequency range [56]. This kind of nanogenerators has exhibited high output together with simple and low-cost fabrication process without any microfabrication process and can be considered as a rational option for the large-scale fabrication of nanogenerators.

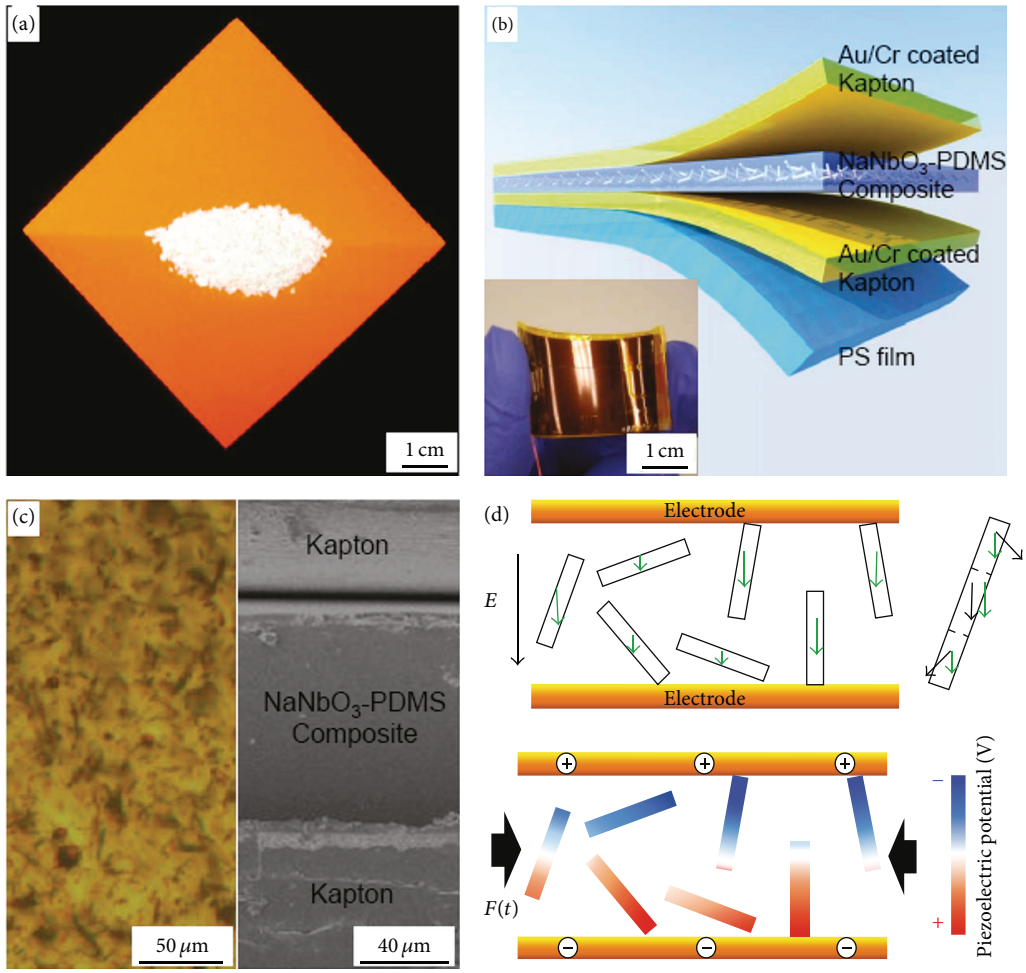

FIGURE 12: The structure and characterization of $NaNbO_3$ nanogenerators. (a) Photograph of $NaNbO_3$ nanowire powder. (b) Structural diagram of the $NaNbO_3$ nanogenerators. (c) AFM and SEM images. (d) The working mechanism of the $NaNbO_3$ nanogenerators. (Reproduced from [9] with the permission from American Chemical Society.)

3.4. Application of Piezoelectric Nanogenerators. In recent years, several research works about the harvesting of different mechanical energies by the piezoelectric nanogenerators have been conducted by researchers, which promoted their practical applications in various fields. For example, the nanogenerators can be used to harvest the biomechanical energies from the bending of a human finger, folding, and releasing of a human elbow, the running motion of a living hamster [63] (Figure 13). Moreover, an *in vivo* nanogenerator that can convert the mechanical energy from the breath and heartbeat of a living rat into electrical outputs have also been reported [65]. Besides the energy from the human and animal bodies, many kinds of mechanical energies in the environment can also be harvested by the nanogenerators, including the mechanical pressures from a moving vehicle [64] and raindrops [66], as well as the vibration induced by liquid and air flows [67–71]. According to the above-mentioned behavior, several kinds of applications based on the piezoelectric nanogenerators have been demonstrated, including the power sources for driving microelectronic devices, the active sensors, the self-powered sensors, and some hybrid cells for energy sources.

3.4.1. Power Source for Driving Electronic Devices. As known, piezoelectric nanogenerators have been viewed as one of the most promising candidates in the microscale power supply systems for driving the microelectronic devices. However, the electrical output of the piezoelectric nanogenerators is actually generated due to the back and forth motion of electrons in the external circuit driving by the piezoelectric potential. Therefore, it is necessary to convert the alternative and impulsive electrical output signals into direct-current (DC) signals to drive the electronic devices, for example, by bridge rectifiers. In the early-stage ZnO nanogenerators, the output voltage and power density are limited. Therefore, a charge storage unit such as a capacitor was usually used for the accumulation of electric energy generated by the nanogenerators. After the charging process, the system can be used for driving some electronic devices, such as LED

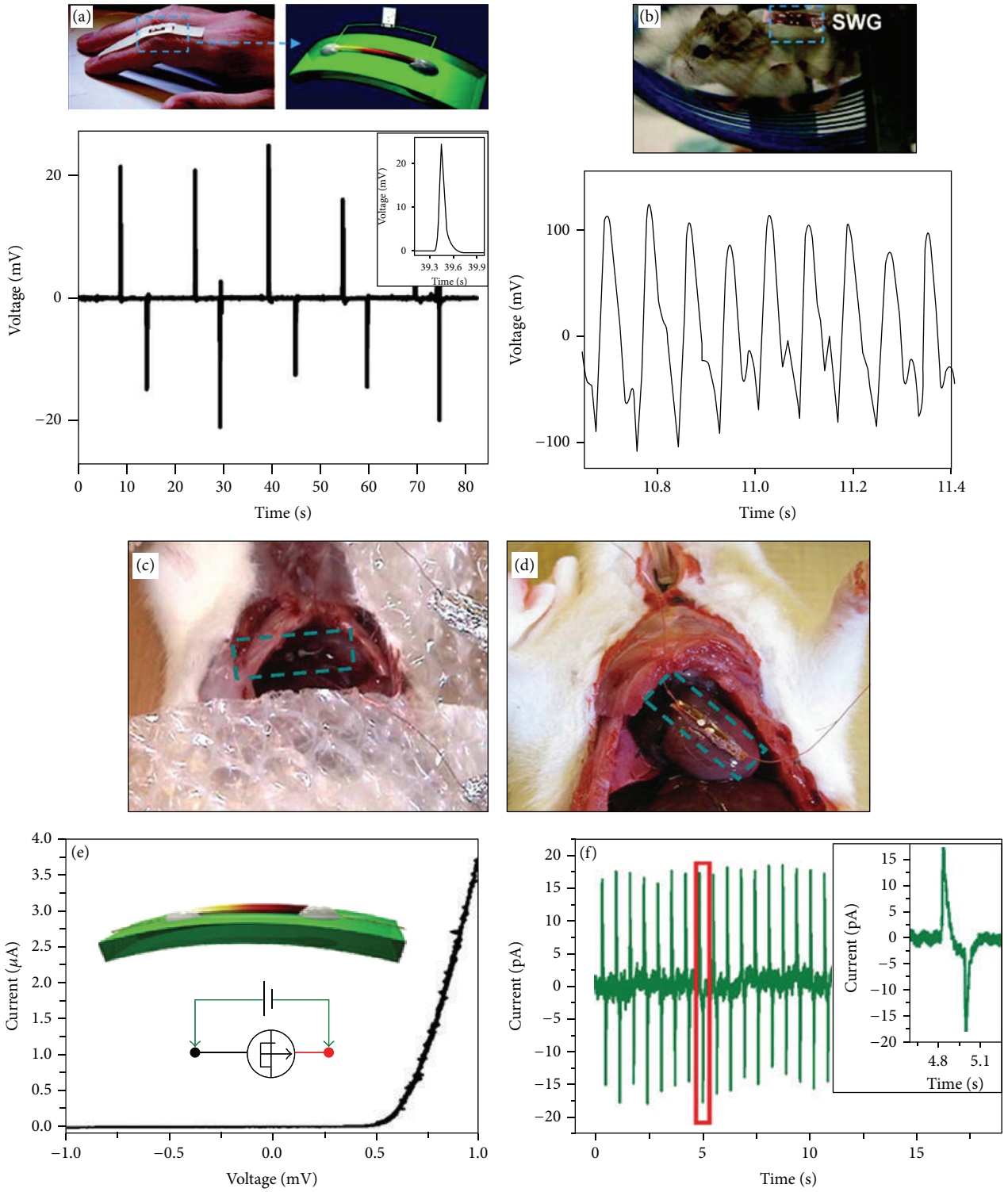

FIGURE 13: The application of single wire nanogenerator for harvesting the biomechanical energies. (a) Finger bending. (b) Hamster running. (c) Rat breath. (d) Rat heartbeat. (e) *I-V* characteristic. (f) Generated current from the heartbeat of rat. [Reproduced from [63, 64] with the permission from American Chemical Society and Copyright WILEY-VCH Verlag GmbH & Co. KGaA, Weinheim.]

and wireless data transmitters [22, 36]. Recently, the output voltage and power density of the nanogenerators have been largely improved by researchers. The output power could meet the requirement of some devices such as the LED and LCD screens. Several nanogenerators based on ZnO or PZT materials have been employed as the power source for such devices without any rectifying and charge storage units, which can simplify the external circuit and decrease the dimension of the system [7, 49, 64]. There are also some research works about the nanogenerators based on piezoelectric thin films for driving the microdevices. For example, Hwang and coworkers have demonstrated a self-powered cardiac pacemaker powered by a flexible single crystalline PMN-PT thin film. The output current and voltage of the flexible film harvester reached 145 μA and 8.2 V, respectively, by harvesting the periodic mechanical motions of bending and unbending [72].

3.4.2. Active Sensors. Many experimental results have proved that the output voltage and current of the nanogenerators are closely related to the applied strain and strain rate. Therefore, the nanogenerators can also be employed as active sensors for the strain-related mechanical matters with voltage/current as the sensing parameters. For example, Hu et al. have integrated a nanogenerator onto a tire's inner surface. The deformation of tire during the moving of vehicles could be harvested and converted into output electric signals. Because the change of tire-pressure and speed of the vehicle may lead to change of the strain and strain rate of the nanogenerator, it can be used as the tire-pressure sensor and speed sensor of the moving vehicle [64]. Lin and coworkers have integrated a nanogenerator onto an elastic spring by growing ZnO nanowire arrays on the surface of the spring. Under a cyclic compressive force applied to the spring, the nanogenerator produced a stable AC output voltage and current, which are linearly responding to the applied weight on the spring. Therefore, the nanogenerator can serve as an active sensor for a self-powered weight measurement [73].

Besides the solid contact between the external load and the nanogenerators, the device can also be used for the sensing of air flows. Zhang et al. have demonstrated a composite nanogenerator which can convert the vortex motion in the atmosphere into electricity [69]. The device can be used to detect the win-speed according to the Karman vortex street principle. Lee et al. used a super-flexible nanogenerator for the harvesting of the energy from the gentle wind, which could also be used as an active deformation sensor for the detecting of both wind and human skin motions [67].

As mentioned above, the free charge carrier inside the piezoelectric nanowires will lead to the polarization screening effect and decrease the piezopotential. This mechanism can also be employed for building active sensors based on the variation of charge carriers, for example, the oxide gas sensor or chemical sensors. Zhu et al. have reported a series of research works about the piezo/active chemical sensors based on ZnO piezoelectric nanowire arrays for detecting the humidity, hydrogen, H_2S, ethanol, and glucose in the environment. Because the adsorption of such chemical matters (H_2 in Figure 14) on the surface of the ZnO will lead to the introduction of free charge carriers to the nanowires, the polarization screening effect will be modified and result in the decrease of output voltage to the external circuit from the nanogenerators [74, 75]. The investigation of such active sensors may largely promote the research on self-powered sensor system and the development of modern sensor networks.

3.4.3. For Driving Self-Powered Sensors. The output voltage and current can be used not only as the active sensing parameters in self-powered sensors, but also as the driving source in several kinds of sensors, in which the input voltage or current will be changed with the sensing parameters of the sensors, especially the resistance-type semiconductor sensors. For example, Xu and coworkers have integrated the ZnO VINGs with a nanowire-based pH sensor and UV sensor, respectively. The partial voltage on the sensor part generated by the VING changed with the resistance of the sensing nanowire both in different pH environment and under the irradiation of the UV light [33]. Wu et al. have also reported the self-powered UV sensor based on nanogenerators with PZT textiles and nanowire, respectively [47, 76].

The difference between the above-mentioned self-powered sensors and the nanogenerator-driven electronic devices is that the former one did not need high electric power density which is essential for the operation in latter ones. By integrating both parts with the output of nanogenerator as both the power source and sensing parameter, the researchers have fabricated completed self-powered sensor systems. For example, Lee et al. have demonstrated a self-powered environment sensor system driven by a nanogenerator [67]. The generated electrical power can light up a LED indicator when the sensor part based on single wall carbon nanotubes is exposed to high concentration of mercury ions in water solution. Li and Xia have integrated ZnO VINGs with both the sensor unit and a wireless transmitter unit [77]. In this system, the signal detected by a phototransistor can be transmitted wirelessly by a single transistor RF transmitter under the driving of the nanogenerator.

3.4.4. Hybrid Cells for Harvesting Multiple Energies. Under the demand of long-term energy needs and sustainable development, devices that can harvest multiple types of energies have also been developed. For example, Hansen and coauthors have integrated the piezoelectric nanogenerators with the enzymatic biofuel cell which can harvest the biochemical energy in biofluid. Both unit can be used for harvesting the energy available *in vivo* and can work simultaneously or individually for boosting output and lifetime [12]. Moreover, Xu and Wang have developed a fully integrated solid-state compact hybrid cell that consisted of an organic solid-state dye-sensitized solar cell (DSSC) and piezoelectric nanogenerator in one compact structure for concurrently harvesting both solar and mechanical energy using a single device. In addition to enhancing the open-circuit voltage, the

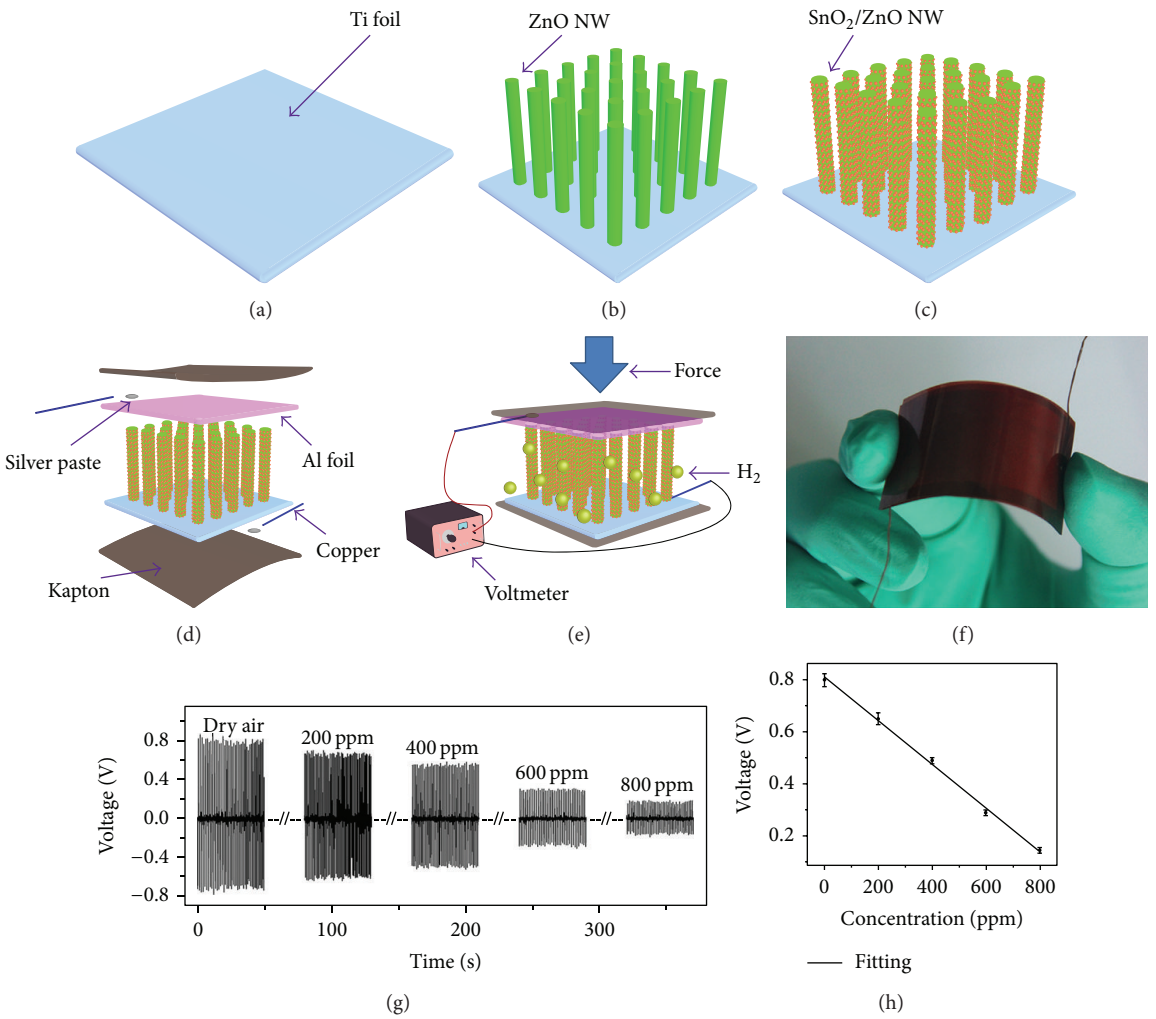

FIGURE 14: The active H_2 sensors based on ZnO VINGs. ((a)–(e)) The schematic diagram of the synthesis process and working mechanism of the sensor. (f) A photograph of the as-fabricated sensor. (g) The output voltage of the sensor with exposure to different concentration of hydrogen gas. (h) The linear relationship between the hydrogen concentration and output voltage. (Reproduced from [16] with the permission from Elsevier.)

hybrid cell can add the total optimum power outputs from both the solar cell and the nanogenerator [78].

4. Future Development of Nanogenerators

Although there have been numerous research works about the fabrication, performance, and application of piezoelectric nanogenerators, the following listed several crucial issues still required to be further improved:

(i) Increase of output power density.

(ii) The integration packaging of energy storage unit with the nanogenerators.

(iii) Optimization on harvesting efficiency of mechanical energy from various working conditions.

(iv) Optimization of electromechanical conversion efficiency through structural design.

(v) Long-term stability, mechanical strength, and chemical stability of the nanogenerators.

Moreover, there are also some problems still required to be solved for the application of nanogenerators, which are listed as follows:

(i) The structural design to guarantee the long-term stability and mechanical strength of the active chemical sensors.

(ii) The harvesting method of mechanical energy to generate stable output voltage for the active sensors, which is crucial for the accuracy of the sensing results.

(iii) The integration and packaging of nanogenerator and sensing unit for the self-powered systems.

(iv) Temperature drift during the sensing process for active/self-powered sensors.

(v) The integration of active or self-powered system with date processing and transmitting systems.

5. Conclusions

In this paper, we provide a comprehensive review of the piezoelectric nanogenerators in the last 8 years. According to the mechanical configuration of the piezoelectric nanowires, there are three major models for the nanogenerators, including the lateral bending model, vertical compression model, and the lateral stretching models. For some devices, the working mechanism of the nanogenerators may be due to the coupling of lateral bending and stretching models. Based on these basic models, three major types of nanogenerators were fabricated by researchers. Among them, the VINGs were mostly investigated due to the higher output and the proven fabrication technique of ZnO nanowire arrays; the LINGs with the highest energy conversion efficiency have also been investigated in recent years with the development of electrospinning techniques; the nanowire-composite type nanogenerators with simplest fabrication process and high electrical output have exhibited great potentials. By harvesting the mechanical energies such as the muscle movement, heartbeats, air/water flow, and solid pressures and rain drops, the nanogenerators can be used as the power source for driving micro/nanodevices and self-powered sensors, as well as the active sensors for the detection the variation of strain-related physical phenomenon and chemical conditions. Moreover, the piezoelectric nanogenerators can be integrated with other energy harvesting devices for building hybrid cells. Although numerous efforts have already been done for promoting the practical application of piezoelectric nanogenerators, there are some critical issues which still need to be further resolved, for example, the energy integration of nanogenerators for high output power sources, the structural design for increasing the energy harvesting efficiency in different conditions, and the development of practicable integrated self-powered systems with improved stability and reliability. Furthermore, the long-term stability and standard testing method of the nanogenerators still need to be concerned in the future studies.

Conflict of Interests

The authors declare that there is no conflict of interests regarding the publication of this paper.

Acknowledgments

The authors thank Professor Yang Luo in East China Normal University for the discussion about the finite element analysis works. This work was financially supported by the National Science Foundation of China (Grant nos. 11474088, 61274073), the National High-Tech Research and Development Program of China (863 Program, Grant no. 2013AA031903), the Applied Basic Research Project of Wuhan (Grant no. 2014010101010006), and the Natural Science Foundation of Hubei Province in China (Grant no. 2014CFB557).

References

[1] F. Patolsky and C. M. Lieber, "Nanowire nanosensors," *Materials Today*, vol. 8, no. 4, pp. 20–28, 2005.

[2] J. Huang and Q. Wan, "Gas sensors based on semiconducting metal oxide one-dimensional nanostructures," *Sensors*, vol. 9, no. 12, pp. 9903–9924, 2009.

[3] H. Yan, H. S. Choe, S. Nam et al., "Programmable nanowire circuits for nanoprocessors," *Nature*, vol. 470, no. 7333, pp. 240–244, 2011.

[4] P. M. Rørvik, T. Grande, and M.-A. Einarsrud, "One-dimensional nanostructures of ferroelectric perovskites," *Advanced Materials*, vol. 23, no. 35, pp. 4007–4034, 2011.

[5] Z. L. Wang, "From nanogenerators to piezotronicsa—a decade-long study of ZnO nanostructures," *MRS Bulletin*, vol. 37, no. 9, pp. 814–827, 2012.

[6] Z. L. Wang and J. Song, "Piezoelectric nanogenerators based on zinc oxide nanowire arrays," *Science*, vol. 312, no. 5771, pp. 242–246, 2006.

[7] L. Gu, N. Cui, L. Cheng et al., "Flexible fiber nanogenerator with 209 v output voltage directly powers a light-emitting diode," *Nano Letters*, vol. 13, no. 1, pp. 91–94, 2013.

[8] J. Kwon, W. Seung, B. K. Sharma, S.-W. Kim, and J.-H. Ahn, "A high performance PZT ribbon-based nanogenerator using graphene transparent electrodes," *Energy and Environmental Science*, vol. 5, no. 10, pp. 8970–8975, 2012.

[9] J. H. Jung, M. Lee, J.-I. Hong et al., "Lead-free $NaNbO_3$ nanowires for a high output piezoelectric nanogenerator," *ACS Nano*, vol. 5, no. 12, pp. 10041–10046, 2011.

[10] C. Falconi, G. Mantini, A. D'Amico, and V. Ferrari, "Modeling of piezoelectric nanodevices," in *Piezoelectric Nanomaterials for Biomedical Applications*, G. Ciofani and A. Menciassi, Eds., Nanomedicine and Nanotoxicology, chapter 4, pp. 93–133, Springer, Berlin, Germany, 2012.

[11] G. Mantini, Y. Gao, A. D'Amico, C. Falconi, and Z. L. Wang, "Equilibrium piezoelectric potential distribution in a deformed ZnO nanowire," *Nano Research*, vol. 2, no. 8, pp. 624–629, 2009.

[12] B. J. Hansen, Y. Liu, R. Yang, and Z. L. Wang, "Hybrid nanogenerator for concurrently harvesting biomechanical and biochemical energy," *ACS Nano*, vol. 4, no. 7, pp. 3647–3652, 2010.

[13] Y. Yang, H. Zhang, Z.-H. Lin et al., "A hybrid energy cell for self-powered water splitting," *Energy and Environmental Science*, vol. 6, no. 8, pp. 2429–2434, 2013.

[14] Y. Zhao, X. Lai, P. Deng et al., "Pt/ZnO nanoarray nanogenerator as self-powered active gas sensor with linear ethanol sensing at room temperature," *Nanotechnology*, vol. 25, no. 11, Article ID 115502, 2014.

[15] Y. Fu, W. Zang, P. Wang, L. Xing, X. Xue, and Y. Zhang, "Portable room-temperature self-powered/active H_2 sensor driven by human motion through piezoelectric screening effect," *Nano Energy*, vol. 8, pp. 34–43, 2014.

[16] P. Han, W. Yan, J. Tian, X. Huang, and H. Pan, "Cut directions for the optimization of piezoelectric coefficients of lead magnesium niobate-lead titanate ferroelectric crystals," *Applied Physics Letters*, vol. 86, no. 5, Article ID 052902, 2005.

[17] K. K. Rajan, M. Shanthi, W. S. Chang, J. Jin, and L. C. Lim, "Dielectric and piezoelectric properties of [0 0 1] and [0 1 1]-poled relaxor ferroelectric PZN–PT and PMN–PT single crystals," *Sensors and Actuators A: Physical*, vol. 133, no. 1, pp. 110–116, 2007.

[18] H. Ohigashi, "Electromechanical properties of polarized polyvinylidene fluoride films as studied by the piezoelectric resonance method," *Journal of Applied Physics*, vol. 47, no. 3, pp. 949–955, 1976.

[19] E. Pukada, "History and recent progress in piezoelectric polymers," *IEEE Transactions on Ultrasonics, Ferroelectrics, and Frequency Control*, vol. 47, no. 6, pp. 1277–1290, 2000.

[20] Z. L. Wang, "Towards self-powered nanosystems: from nanogenerators to nanopiezotronics," *Advanced Functional Materials*, vol. 18, no. 22, pp. 3553–3567, 2008.

[21] Y. Qin, X. Wang, and Z. L. Wang, "Microfibre-nanowire hybrid structure for energy scavenging," *Nature*, vol. 451, no. 7180, pp. 809–813, 2008.

[22] G. Zhu, R. Yang, S. Wang, and Z. L. Wang, "Flexible high-output nanogenerator based on lateral ZnO nanowire array," *Nano Letters*, vol. 10, no. 8, pp. 3151–3155, 2010.

[23] Z. Wang, Y. Hu, W. Wang, D. Zhou, Y. Wang, and H. Gu, "Electromechanical conversion behavior of $K_{0.5}Na_{0.5}NbO_3$ nanorods synthesized by hydrothermal method," *Integrated Ferroelectrics*, vol. 142, no. 1, pp. 24–30, 2013.

[24] Z. L. Wang, R. Yang, J. Zhou et al., "Lateral nanowire/nanobelt based nanogenerators, piezotronics and piezo-phototronics," *Materials Science and Engineering R: Reports*, vol. 70, no. 3–6, pp. 320–329, 2010.

[25] Y. Gao and Z. L. Wang, "Equilibrium potential of free charge carriers in a bent piezoelectric semiconductive nanowire," *Nano Letters*, vol. 9, no. 3, pp. 1103–1110, 2009.

[26] C. Falconi, G. Mantini, A. D'Amico, and Z. L. Wang, "Studying piezoelectric nanowires and nanowalls for energy harvesting," *Sensors and Actuators B: Chemical*, vol. 139, no. 2, pp. 511–519, 2009.

[27] Y.-F. Lin, J. Song, Y. Ding, S.-Y. Lu, and Z. L. Wang, "Alternating the output of a CdS nanowire nanogenerator by a white-light-stimulated optoelectronic effect," *Advanced Materials*, vol. 20, no. 16, pp. 3127–3130, 2008.

[28] C.-T. Huang, J. Song, W.-F. Lee et al., "GaN nanowire arrays for high-output nanogenerators," *Journal of the American Chemical Society*, vol. 132, no. 13, pp. 4766–4771, 2010.

[29] Y.-F. Lin, J. Song, Y. Ding, S.-Y. Lu, and Z. L. Wang, "Piezoelectric nanogenerator using CdS nanowires," *Applied Physics Letters*, vol. 92, no. 2, Article ID 022105, 2008.

[30] M.-Y. Lu, J. Song, M.-P. Lu, C.-Y. Lee, L.-J. Chen, and Z. L. Wang, "ZnO–ZnS heterojunction and ZnS nanowire arrays for electricity generation," *ACS Nano*, vol. 3, no. 2, pp. 357–362, 2009.

[31] C.-T. Huang, J. Song, C.-M. Tsai et al., "Single-inn-nanowire nanogenerator with upto 1 v output voltage," *Advanced Materials*, vol. 22, no. 36, pp. 4008–4013, 2010.

[32] X. Wang, J. Song, J. Liu, and Z. L. Wang, "Direct-current nanogenerator driven by ultrasonic waves," *Science*, vol. 316, no. 5821, pp. 102–105, 2007.

[33] S. Xu, Y. Qin, C. Xu, Y. Wei, R. Yang, and Z. L. Wang, "Self-powered nanowire devices," *Nature Nanotechnology*, vol. 5, no. 5, pp. 366–373, 2010.

[34] K.-H. Kim, K. Y. Lee, J.-S. Seo, B. Kumar, and S.-W. Kim, "Paper-based piezoelectric nanogenerators with high thermal stability," *Small*, vol. 7, no. 18, pp. 2577–2580, 2011.

[35] D. Choi, M.-Y. Choi, W. M. Choi et al., "Fully rollable transparent nanogenerators based on graphene electrodes," *Advanced Materials*, vol. 22, no. 19, pp. 2187–2192, 2010.

[36] Y. Hu, Y. Zhang, C. Xu, L. Lin, R. L. Snyder, and Z. L. Wang, "Self-powered system with wireless data transmission," *Nano Letters*, vol. 11, no. 6, pp. 2572–2577, 2011.

[37] Y. Hu, L. Lin, Y. Zhang, and Z. L. Wang, "Replacing a battery by a nanogenerator with 20 v output," *Advanced Materials*, vol. 24, no. 1, pp. 110–114, 2012.

[38] T. T. Pham, K. Y. Lee, J.-H. Lee et al., "Reliable operation of a nanogenerator under ultraviolet light via engineering piezoelectric potential," *Energy and Environmental Science*, vol. 6, no. 3, pp. 841–846, 2013.

[39] G. Zhu, A. C. Wang, Y. Liu, Y. Zhou, and Z. L. Wang, "Functional electrical stimulation by nanogenerator with 58 v output voltage," *Nano Letters*, vol. 12, no. 6, pp. 3086–3090, 2012.

[40] S. Xu, B. J. Hansen, and Z. L. Wang, "Piezoelectric-nanowire-enabled power source for driving wireless microelectronics," *Nature communications*, vol. 1, article 93, 2010.

[41] P. G. Kang, B. K. Yun, K. D. Sung et al., "Piezoelectric power generation of vertically aligned lead-free $(K,Na)NbO_3$ nanorod arrays," *RSC Advances*, vol. 4, no. 56, pp. 29799–29805, 2014.

[42] R. Yang, Y. Qin, L. Dai, and Z. L. Wang, "Power generation with laterally packaged piezoelectric fine wires," *Nature Nanotechnology*, vol. 4, no. 1, pp. 34–39, 2009.

[43] J. Chang, M. Dommer, C. Chang, and L. Lin, "Piezoelectric nanofibers for energy scavenging applications," *Nano Energy*, vol. 1, no. 3, pp. 356–371, 2012.

[44] Z. Wang, J. Hu, A. P. Suryavanshi, K. Yum, and M.-F. Yu, "Voltage generation from individual $BaTiO_3$ nanowires under periodic tensile mechanical load," *Nano Letters*, vol. 7, no. 10, pp. 2966–2969, 2007.

[45] Z. Wang, H. Gu, Y. Hu et al., "Synthesis, growth mechanism and optical properties of (K,Na)NbO3 nanostructures," *CrystEngComm*, vol. 12, no. 10, pp. 3157–3162, 2010.

[46] X. Chen, S. Xu, N. Yao, and Y. Shi, "1.6 V nanogenerator for mechanical energy harvesting using PZT nanofibers," *Nano Letters*, vol. 10, no. 6, pp. 2133–2137, 2010.

[47] W. Wu, S. Bai, M. Yuan, Y. Qin, Z. L. Wang, and T. Jing, "Lead zirconate titanate nanowire textile nanogenerator for wearable energy-harvesting and self-powered devices," *ACS Nano*, vol. 6, no. 7, pp. 6231–6235, 2012.

[48] H. B. Kang, J. Chang, K. Koh, L. Lin, and Y. S. Cho, "High quality Mn-doped $(Na,K)NbO_3$ nanofibers for flexible piezoelectric nanogenerators," *ACS Applied Materials & Interfaces*, vol. 6, no. 13, pp. 10576–10582, 2014.

[49] Y. Hu, Y. Zhang, C. Xu, G. Zhu, and Z. L. Wang, "High-output nanogenerator by rational unipolar assembly of conical nanowires and its application for driving a small liquid crystal display," *Nano Letters*, vol. 10, no. 12, pp. 5025–5031, 2010.

[50] L. Lin, C.-H. Lai, Y. Hu et al., "High output nanogenerator based on assembly of GaN nanowires," *Nanotechnology*, vol. 22, no. 47, Article ID 475401, 2011.

[51] Z.-H. Lin, Y. Yang, J. M. Wu, Y. Liu, F. Zhang, and Z. L. Wang, "$BaTiO_3$ nanotubes-based flexible and transparent nanogenerators," *Journal of Physical Chemistry Letters*, vol. 3, no. 23, pp. 3599–3604, 2012.

[52] J. M. Wu, C. Xu, Y. Zhang, Y. Yang, Y. Zhou, and Z. L. Wang, "Flexible and transparent nanogenerators based on a composite of lead-free $ZnSnO_3$ triangular-belts," *Advanced Materials*, vol. 24, no. 45, pp. 6094–6099, 2012.

[53] B. K. Yun, Y. K. Park, M. Lee et al., "Lead-free $LiNbO_3$ nanowire-based nanocomposite for piezoelectric power generation," *Nanoscale Research Letters*, vol. 9, no. 1, article 4, 2014.

[54] J. H. Jung, C.-Y. Chen, B. K. Yun et al., "Lead-free $KNbO_3$ ferroelectric nanorod based flexible nanogenerators and capacitors," *Nanotechnology*, vol. 23, no. 37, Article ID 375401, 2012.

[55] S. Xu, Y.-W. Yeh, G. Poirier, M. C. McAlpine, R. A. Register, and N. Yao, "Flexible piezoelectric PMN-PT nanowire-based nanocomposite and device," *Nano Letters*, vol. 13, no. 6, pp. 2393–2398, 2013.

[56] Z. Zhou, H. Tang, and H. A. Sodano, "Scalable synthesis of morphotropic phase boundary lead zirconium titanate nanowires for energy harvesting," *Advanced Materials*, vol. 26, pp. 7547–7554, 2014.

[57] B.-S. Lee, B. Park, H.-S. Yang et al., "Effects of substrate on piezoelectricity of electrospun poly(vinylidene fluoride)-nanofiber-based energy generators," *ACS Applied Materials & Interfaces*, vol. 6, no. 5, pp. 3520–3527, 2014.

[58] C. Chang, V. H. Tran, J. Wang, Y.-K. Fuh, and L. Lin, "Direct-write piezoelectric polymeric nanogenerator with high energy conversion efficiency," *Nano Letters*, vol. 10, no. 2, pp. 726–731, 2010.

[59] C. Jiyoung and L. Liwei, "Large array electrospun PVDF nanogenerators on a flexible substrate," in *Proceedings of the 16th International Solid-State Sensors, Actuators and Microsystems Conference (TRANSDUCERS '11)*, pp. 747–750, June 2011.

[60] Z. Pi, J. Zhang, C. Wen, Z.-B. Zhang, and D. Wu, "Flexible piezoelectric nanogenerator made of poly(vinylidenefluoride-co-trifluoroethylene) (PVDF-TrFE) thin film," *Nano Energy*, vol. 7, pp. 33–41, 2014.

[61] L. Persano, C. Dagdeviren, Y. Su et al., "High performance piezoelectric devices based on aligned arrays of nanofibers of poly(vinylidenefluoride-co-trifluoroethylene)," *Nature Communications*, vol. 4, article 1633, 2013.

[62] W. Zeng, X.-M. Tao, S. Chen, S. Shang, H. L. W. Chan, and S. H. Choy, "Highly durable all-fiber nanogenerator for mechanical energy harvesting," *Energy and Environmental Science*, vol. 6, no. 9, pp. 2631–2638, 2013.

[63] R. Yang, Y. Qin, C. Li, G. Zhu, and Z. L. Wang, "Converting biomechanical energy into electricity by a muscle-movement-driven nanogenerator," *Nano Letters*, vol. 9, no. 3, pp. 1201–1205, 2009.

[64] Y. Hu, C. Xu, Y. Zhang, L. Lin, R. L. Snyder, and Z. L. Wang, "A nanogenerator for energy harvesting from a rotating tire and its application as a self-powered pressure/speed sensor," *Advanced Materials*, vol. 23, no. 35, pp. 4068–4071, 2011.

[65] Z. Li, G. Zhu, R. Yang, A. C. Wang, and Z. L. Wang, "Muscle-driven in vivo nanogenerator," *Advanced Materials*, vol. 22, no. 23, pp. 2534–2537, 2010.

[66] R. Guigon, J.-J. Chaillout, T. Jager, and G. Despesse, "Harvesting raindrop energy: experimental study," *Smart Materials and Structures*, vol. 17, no. 1, Article ID 015039, 2008.

[67] S. Lee, S.-H. Bae, L. Lin et al., "Super-flexible nanogenerator for energy harvesting from gentle wind and as an active deformation sensor," *Advanced Functional Materials*, vol. 23, no. 19, pp. 2445–2449, 2013.

[68] D.-A. Wang and H.-H. Ko, "Piezoelectric energy harvesting from flow-induced vibration," *Journal of Micromechanics and Microengineering*, vol. 20, no. 2, Article ID 025019, 2010.

[69] R. Zhang, L. Lin, Q. Jing et al., "Nanogenerator as an active sensor for vortex capture and ambient wind-velocity detection," *Energy and Environmental Science*, vol. 5, no. 9, pp. 8528–8533, 2012.

[70] C. Sun, J. Shi, D. J. Bayerl, and X. Wang, "PVDF microbelts for harvesting energy from respiration," *Energy and Environmental Science*, vol. 4, no. 11, pp. 4508–4512, 2011.

[71] Z. Li and Z. L. Wang, "Air/liquid-pressure and heartbeat-driven flexible fiber nanogenerators as a micro/nano-power source or diagnostic sensor," *Advanced Materials*, vol. 23, no. 1, pp. 84–89, 2011.

[72] G.-T. Hwang, H. Park, J.-H. Lee et al., "Self-powered cardiac pacemaker enabled by flexible single crystalline PMN-PT piezoelectric energy harvester," *Advanced Materials*, vol. 26, pp. 4880–4887, 2014.

[73] L. Lin, Q. Jing, Y. Zhang et al., "An elastic-spring-substrated nanogenerator as an active sensor for self-powered balance," *Energy & Environmental Science*, vol. 6, no. 4, pp. 1164–1169, 2013.

[74] D. Zhu, Y. Fu, W. Zang, Y. Zhao, L. Xing, and X. Xue, "Piezo/active humidity sensing of CeO_2/ZnO and SnO_2/ZnO nanoarray nanogenerators with high response and large detecting range," *Sensors and Actuators B*, vol. 205, pp. 12–19, 2014.

[75] R. Yu, C. Pan, J. Chen, G. Zhu, and Z. L. Wang, "Enhanced performance of a ZnO nanowire-based self-powered glucose sensor by piezotronic effect," *Advanced Functional Materials*, vol. 23, no. 47, pp. 5868–5874, 2013.

[76] S. Bai, Q. Xu, L. Gu, F. Ma, Y. Qin, and Z. L. Wang, "Single crystalline lead zirconate titanate (PZT) nano/micro-wire based self-powered UV sensor," *Nano Energy*, vol. 1, no. 6, pp. 789–795, 2012.

[77] D. Li and Y. Xia, "Electrospinning of nanofibers: reinventing the wheel?" *Advanced Materials*, vol. 16, no. 14, pp. 1151–1170, 2004.

[78] C. Xu and Z. L. Wang, "Compact hybrid cell based on a convoluted nanowire structure for harvesting solar and mechanical energy," *Advanced Materials*, vol. 23, no. 7, pp. 873–877, 2011.